

Two-Dimensional Zeolites: Current Status and Perspectives

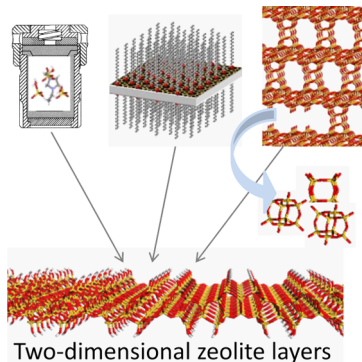
Wiesław J. Roth,^{†,||} Petr Nachtigall,[‡] Russell E. Morris,[§] and Jiří Čejka*,[†]

[†]J. Heyrovský Institute of Physical Chemistry, Academy of Sciences of the Czech Republic, v.v.i., Dolejškova 3, CZ-182 23 Prague 8, Czech Republic

[‡]Department of Physical and Macromolecular Chemistry, Faculty of Science, Charles University in Prague, Hlavova 2030, Prague 2, 128 00, Czech Republic

[§]EaStCHEM School of Chemistry, University of St. Andrews, St. Andrews KY16 9ST, Scotland

^{||}Faculty of Chemistry, Jagiellonian University in Kraków, ul. Ingardena 3,30-060 Kraków, Poland



CONTENTS

1. Introduction	4807
2. Early Discoveries Relevant to Layered Zeolite Materials	4808
3. Layered Zeolite Materials: General Overview	4809
4. Synthesis of Layered Zeolite Precursors and Other Primary Lamellar Zeolite Forms	4812
4.1. Hydrothermal Synthesis of Lamellar Precursors	4813
4.2. Surfactant-Assisted Synthesis of Nanosheet Zeolites	4815
4.3. Two-Dimensional Zeolites Synthesized on Metal Supports	4816
4.4. Three- to Two-Dimensional Transformation of Parent Zeolites	4816
4.5. Assembly–Disassembly–Organization–Reassembly Strategy	4816
5. Postsynthetic Modification of Layered Zeolite Precursors	4817
5.1. Precursor Detemplation	4817
5.2. Expansion of Interlamellar Space	4818
5.3. Stabilizing Interlayer Expanded Precursors	4819
5.4. Pillaring	4820
6. Delamination and Exfoliation	4822
6.1. MWW Family	4822
6.2. Other Delaminated Zeolites	4823
6.3. Colloidal Suspensions of Zeolite Nanosheets	4824
7. Structure of Lamellar Materials	4824
7.1. X-ray Powder Diffraction and Electron Diffraction	4824
7.2. Modeling of 2D Zeolites	4825
7.2.1. Application of Force Fields	4825

7.2.2. Application of Density Functional Theory Methods	4825
8. Two-Dimensional Zeolites in Catalysis	4827
8.1. Petrochemistry	4828
8.2. Oxidation Reactions	4829
8.3. Fine Chemical Synthesis	4830
8.4. Organometallics	4830
9. Challenges and Opportunities	4830
Author Information	4832
Notes	4832
Biographies	4832
Acknowledgments	4833
References	4833

1. INTRODUCTION

Zeolites are well-known as valuable crystalline solids with framework structures containing discrete micropores of molecular dimensions that accommodate exchangeable extra-framework cation sites.^{1–3} In terms of host–guest interactions, zeolites can be viewed as host frameworks with structurally intact and immutable three-dimensional (3D) structures. They show exceptional catalytic and sorption characteristics together with very desirable environmental qualities.^{4–7} Zeolites are widely used in commercial applications as catalysts for hydrocarbon conversions in petroleum and chemical industries,^{8–10} as sorbents for small-molecule separation processes, and as ion exchangers in detergents.¹¹

The remarkable properties of zeolites are closely related to their structural features.¹² Zeolites are composed of corner-sharing TO_4 tetrahedra, with T standing for tetrahedrally coordinated framework atoms, such as Si and Al or other heteroatoms.^{12,13} Zeolites contain one-, two-, or three-dimensional systems of channels, which are interconnected in a number of different ways. The topological uniqueness of individual zeolite structures is defined by coordination sequences and vertex symbols.¹⁴ The number of possible zeolites is (theoretically) unlimited;^{15–19} however, only 213 different framework structures are accepted so far by the Structural Commission of the International Zeolite Association and have obtained a unique three-letter code.^{14,20} Most of the synthetic zeolites were obtained via solvothermal synthesis by use of different reaction conditions, reactants, and structure-

Received: November 1, 2013

Published: February 21, 2014

directing agents (SDA); some of them were obtained via solvent-free synthesis.²¹ The reaction proceeds either directly to 3D zeolites (in most cases) or it can proceed via a two-dimensional (2D) layered zeolite precursor, LZP (about 10 cases; see Figure 1). Recently, it has been shown that new

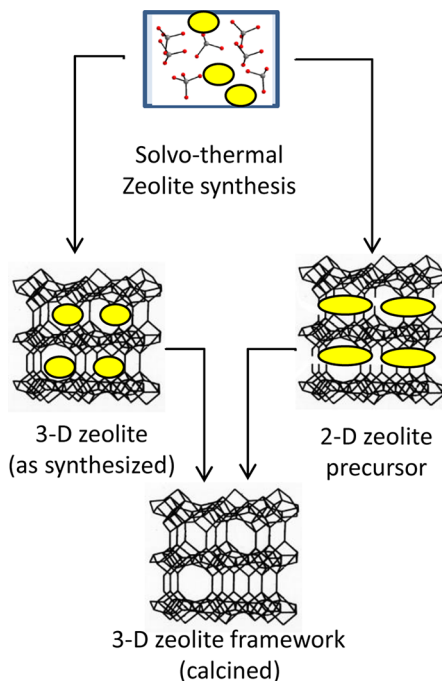


Figure 1. Schematic representation of zeolite solvothermal synthesis. A variety of reaction conditions (temperature, pressure, and reaction time) and different reactants and structure-directing agents (depicted in yellow) led to the formation (in nature or by synthesis) of 213 different structural types of zeolites. In about 200 cases, reaction appears to proceed directly to 3D zeolite structure (left pathway); in about 10 cases (including some obtained by the above direct method), the 2D zeolite precursors were found to be formed before the condensation of individual layers to 3D zeolite (right pathway).

zeolites can be obtained by a completely different mechanism: removal or replacement of structural units of an already synthesized 3D zeolite.^{22,23}

Zeolites have been traditionally viewed as covalently bonded continuous frameworks extended in three dimensions.^{14,24,25} To take account of the aforementioned layered intermediates LZP, which may also have similar porosity and structure to zeolites, this definition may be extended to include so-called “2D zeolites”, where the structures propagate in only two dimensions.^{2,26,27} These 2D LZP produce the standard 3D zeolite frameworks by topotactic condensation induced by calcination, but they could also be modified into other types of structures, particularly expanded ones, by swelling, pillaring, or stabilization.²⁸ The onset of this new paradigm is linked to the first synthesis of MWW zeolites, specifically MCM-22,^{29,30} and many LZP have been synthesized and described in the past decade.^{31,32}

The synthesis of zeolites with new structures, in particular those with large channels where bigger molecules can diffuse into the zeolite crystallite, is an active field of research. Germanosilicate ITQ-37³³ is a zeolite with the largest channel diameter (20 Å) synthesized so far. The synthesis of zeolites containing both micropores and mesopores is also actively researched.^{34,35} The advantage of hierarchical zeolites is that

diffusion is enhanced in the mesopores. A number of different strategies have been proposed, including postsynthetic treatments with mild acids or bases resulting in partial dissolution of framework atoms, mechanical hole drilling, or various postsynthetic treatments of 2D layered zeolite precursors.^{26,36,37} A subset of this field, hierarchical materials based on two-dimensional zeolites, is primarily discussed in this review. For discussions of the aspects of zeolite synthesis and hierarchical zeolites in general, the reader is referred to relevant literature.^{38,39}

The history of layered zeolite materials is briefly discussed in section 2, and the traditional concept of 3D zeolites is expanded in section 3 based on some recently proposed generalization.⁴⁰ The synthesis of layered zeolite precursors and other primary lamellar zeolite forms is discussed in section 4, followed by aspects of postsynthetic modification, delamination, structural characterization, and catalytic properties. Finally, the challenges and perspectives facing this relatively young emerging field are discussed and future areas of potential interest are considered.

2. EARLY DISCOVERIES RELEVANT TO LAYERED ZEOLITE MATERIALS

The key revelation in the field of layered zeolites was the discovery that the synthesis of MCM-22 (MWW topology) can proceed along two different pathways: (i) direct synthesis, as in the standard zeolites (MCM-49),^{41,42} or (ii) via layered precursor (MCM-22P, Figure 1). The existence of MCM-22P layers was corroborated by swelling and pillaring studies, resulting in the zeolite material MCM-36.⁴³ The results concerning various forms of zeolite MWW were initially disclosed in patents and later in the scientific literature.^{29,41,44,45} The layered 2D character was also demonstrated early on for ERB-1,⁴⁶ which is a boron analogue of MCM-22. Other zeolites synthesized independently in the 1980s and early 1990s have been considered related (isostructural) to MCM-22: PSH-3,⁴⁷ SSZ-25,⁴⁸ and ERB-1.⁴⁹

The discovery of a layered precursor to an established 3D zeolite, FER (known in both natural and synthetic forms),^{50–52} was another milestone in the field. The layered ferrierite precursor was also amenable to expansion by swelling and delamination.⁵³ This opened up the possibility that formation of 3D zeolites from layered precursors was a more general alternative to direct synthesis, and in principle it appears possible for all zeolites.² These fundamental breakthroughs presented new opportunities in the field of large-pore zeolites by showing pathways toward expanded zeolite structures with increased accessibility to intrinsically strong acid centers, even for bulkier molecules.

Owing to the central role of MCM-22P in the field of layered zeolite materials, the most important achievements are briefly reviewed below as an example of what can be achieved. Much of this work has been replicated with other frameworks; the corresponding materials are presented in Figure 2. The layered MCM-22 precursor, MCM-22P, comprises nanosheets having the MWW topology with uniform thickness of 2.5 nm stacked in register (aligned vertically) with an overall stacking repeat about 0.2 nm greater than in the final 3D framework. The alignment of layers indicating 3D order is concluded on the basis of observation of well-defined interlayer reflections [Miller indices (hkl) with nonzero l and (h or k)]. The layers are interconnected via hydrogen bonding between silanol groups, with the possible involvement of hexamethylenimine template molecules that are occluded between the layers.

Layer ordering	Type of material	Material Name
	Ordered (multi)-layered precursor	MCM-22P
	3D Framework	MCM-22
	Disordered (multi)-layered precursor	EMM-10P
	Mono-layer delaminated	MCM-56
	Detemplated sub-zeolite	MCM-56 analogue
	Swollen precursor	
	Stabilized ordered precursor (IEZ)	IEZ-MWW
	Stabilized disordered precursor (IEZ)	EMM-12
	Pillared zeolite	MCM-36
	Organic pillared zeolite	MCM-22-BETB
	Delaminated swollen precursor	ITQ-2
	Colloidal suspension	

Figure 2. MWW (MCM-22) monolayers provide a variety of materials by direct synthesis (top four) and by postsynthetic modifications. Schematic representations of individual types of materials obtained from MCM-22P are shown, along with the material names (corresponding references can be found in Table 1).

The layered MCM-22P precursor is in effect a 2D solid⁵⁴ consisting of zeolite monolayers. This fundamental discovery of layered zeolite precursors had profound implications, since 2D solids have been known to allow structural postsynthetic modifications, including interlayer expansion leading to enhanced porosity. These types of materials were exemplified previously by swollen and pillared clays.^{55–57} MCM-22P was immediately exploited in this direction,⁴³ albeit with some initial challenges requiring innovative solutions to overcome swelling problems, as will be elaborated below.

The MCM-22P nanosheet assemblies can be processed in practice in a number of different ways, leading to various materials reviewed in Figure 2. The conventional calcination of MCM-22P leads to regular 3D zeolite framework MCM-22. While in MCM-22P the individual layers are stacked in an ordered manner, materials with disordered layer stacking (EMM-10P)⁵⁸ and delaminated layers (MCM-56)^{45,59} were also obtained. In addition, a “MCM-56 analogue” was prepared upon treatment of MCM-22P with an acid, causing apparent removal of species (detemplation) from the interlayer region.^{60,61} While MCM-22P contracts upon calcination, its initial slight expansion (~ 0.2 nm) can be preserved upon stabilization with a suitable silica source leading to interlayer expanded zeolite (IEZ) material with ordered (IEZ-MWW)^{62,63} and disordered (EMM-12)⁶⁴ layer stacking. The MCM-22P precursor can be expanded with a basal spacing increase by 2 nm and more upon swelling and subsequently transformed into materials with increased interlayer porosity in a number of ways. The swollen precursor has also been pillared, by use of either silica (MCM-36)⁴³ or organic pillars (MCM-22-BETB).⁶⁵ Last but not least, the transformation of swollen precursor into delaminated swollen precursor ITQ-2⁶⁶ and into colloidal suspension has been reported.⁶⁷

Compared with zeolites, conventional 2D layered solids had been generally less active and less likely to exhibit size and shape selectivity in catalytic reactions. They were still found attractive and of interest for commercial use because of their availability and cost, exemplified by clays. The layered zeolite precursor MCM-22P proved its perceived potential in the pillared form as MCM-36 by showing superior catalytic activity in some catalytic processes.⁶⁸ Subsequently, a number of new layered zeolite precursors and corresponding postsynthetically modified materials have been reported in the past decade. Figure 3 presents the list of approved zeolite frameworks provided by the IZA Structure Commission; those with proven layered forms are highlighted, and in addition, zeolites of particular commercial interest¹⁰ are shown in red.

3. LAYERED ZEOLITE MATERIALS: GENERAL OVERVIEW

The achievements described above opened new fundamental opportunities for the synthesis of novel zeolitic materials with rich application potential.²⁷ The development can be described as an expansion in three main directions. (i) Additional zeolite frameworks were found to be formed via a layered zeolite precursor (LZP), for example, FER, SOD, MFI, NSI, and PCR; see section 4.1 for a full account and more detailed discussion. (ii) New types of layered structures were prepared by direct synthesis, for example, delaminated MCM-56⁴⁵ and disordered EMM-10P as additional examples of the MWW family (Figure 2), while self-pillared zeolite structure was reported for MFI (pillars separating the individual layers are formed during the synthesis without addition of any pillarizing agent).⁶⁹ (iii)

ABW	ACO	AEI	AEL	AEN	AET	AFG	AFI	AFN	AFO	AFR	AFS
AFT	AFX	AFY	AHT	ANA	APC	APD	AST	ASV	ATN	ATO	ATS
ATT	ATV	AWO	AWW	BCT	*BEA	BEC	BIK	BOF	BOG	BOZ	BPH
BRE	BSV	CAN	CAS	CDO	CFI	CGF	CGS	CHA	-CHI	-CLO	CON
CZP	DAC	DDR	DFO	DFT	DOH	DON	EAB	EDI	EMT	EON	EPI
ERI	ESV	ETR	EUO	EZT	FAR	FAU	FER	FRA	GIS	GIU	GME
GON	GOO	HEU	IFO	IFR	IHW	IMF	IRR	ISV	ITE	ITH	ITR
ITT	-ITV	ITW	IWR	IWS	IWW	IWW	JBW	JOZ	JRY	JSN	JSR
JST	JSW	KFI	LAU	LEV	LIO	-LIT	LOS	LOV	LTA	LTF	LTJ
LTL	LTN	MAR	MAZ	MEI	MEL	MEP	MER	MFI	MFS	MON	MOR
MOZ	*MRE	MSE	MSO	MTF	MTN	MTT	MTW	MVY	MWW	NAB	NAT
NES	NON	NPO	NPT	NSI	OBW	OFF	OKO	OSI	OSO	OWE	-PAR
PAU	PCR	PHI	PON	PUN	RHO	-RON	RRO	RSN	RTE	RTH	RUT
RWR	RWY	SAF	SAO	SAS	SAT	SAV	SBE	SBN	SBS	SBT	SEW
SFE	SFF	SFG	SFH	SFN	SFO	SFS	*SFV	SFW	SGT	SIV	SOD
SOF	SOS	SSF	SSY	STF	STI	*STO	STT	STW	-SVR	SVV	SZR
TER	THO	TOL	TON	TSC	TUN	UEI	UFI	UOS	UOZ	USI	UTL
UWY	VET	VFI	VNI	VSV	WEI	-WEN	YUG	ZON			MCM-41

16	ZEO	Synthetic used industrially or of commercial interest (ref. 10)
13	ZEO	Layered or 2D form known
3	ZEO	Used commercially and layered or 2D form known

Figure 3. Zeolites with known 2D forms (yellow box with bold frame) and zeolites used industrially or of commercial interest (red bold 3-letter code) based on reference 10 in the context of the approved 213 zeolite frameworks plus the mesoporous MCM-41 material.

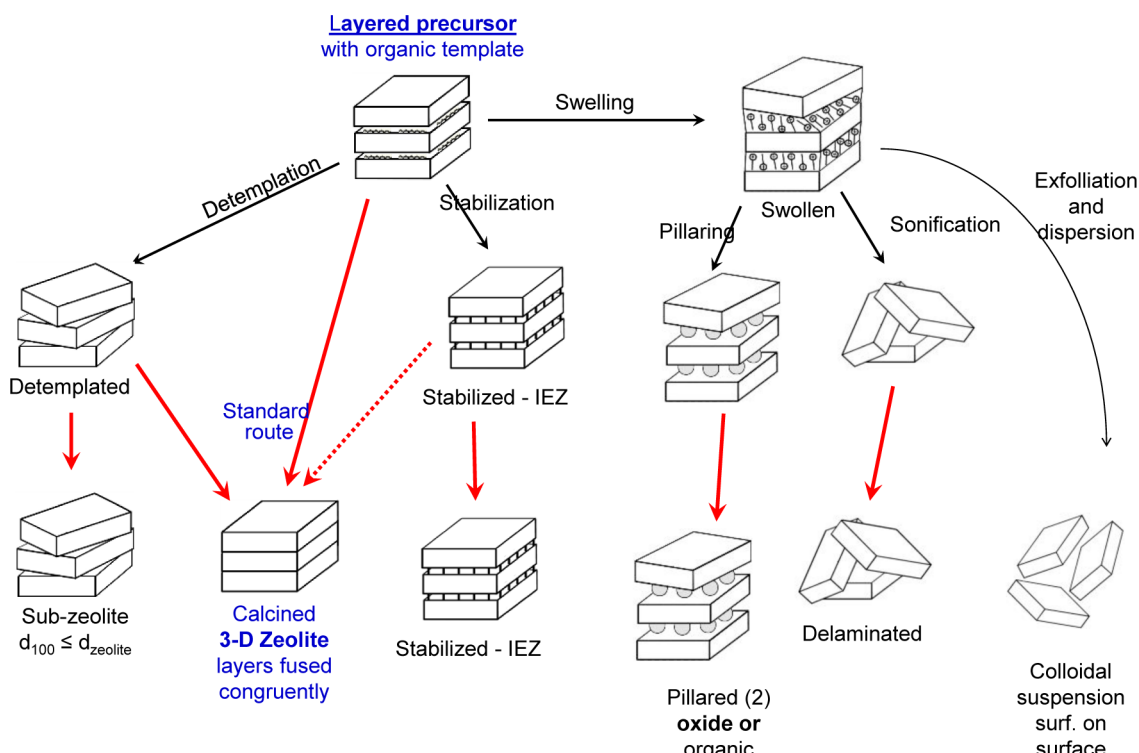


Figure 4. Schematic representation of possible postsynthetic manipulations with layered zeolite precursors, LZP (red arrows denote the calcination). LZP can be either detemplated, stabilized, swollen, or directly calcined (“standard route” leading to the 3D zeolite). A detemplation leads to the detemplated material that can be subsequently calcined leading either to the 3D zeolite or to subzeolite. Stabilization of LZP (using a suitable source of silica) leads to stabilized interlayer expanded zeolite (IEZ) that can be subsequently calcined. The swollen LZP material can be further treated: pillaring and subsequent calcination leads to pillared material, sonification and subsequent calcination may lead to delaminated material, and exfoliation and dispersion provides colloidal suspension of nanosheets.

Table 1. Compilation of Layered Zeolite Forms^a

		common layer ^b				common layer ^b				from UTI ^c			
		MFI	FER	CDO	CAS	MCM-65 ^{86,87}	CDS-1 MCM-65 ^{86,87}	CAS ^{263,c}	NU-6(2) ^{79,264}	RRO	HEU	SOD	RWR
													PCR
3D framework	MCM-49 ^{41,42,c}	ZSM-5 ^{62,c}	FER ^{80,c}							RUB-41 ²⁶⁵	HEU ^{266,c}	SOD ^{267,c}	RUB-24 ⁹³
ordered (multi)layered precursor	MCM-22P, ERB-1 ^{29,30,46,c}	preFER ^{2,c}	preFER ^{2,c}	PLS-1 MCM-65 ^{86,87,c}	Partial ⁸⁰	NU-6(1) ^{79,264,c}				RUB-39 ^{265,c}			IPC-4 ²³
disordered (multi)layered precursor monolayer; delaminated	EMM-10P ^{58,c}					EU-19 ^{268,c}							COK-14 ²²
multilamellar precursor w/ surfactant (single-unit-cell nanosheets)	MCM-56 ^{59,c}												AFO ^{94,c}
unilamellar precursor w/ surfactant detemplated/subzeolite	MCM-56 analogue ⁶³	88 ⁸⁹											
stabilized ordered precursor (IEZ)	MWW-1EZ ⁶²	74 ^c											
stabilized disordered precursor (IEZ) swollen precursor	EMM-12 ⁶⁴	63											
delaminated swollen precursor	ITQ-2 ⁶⁶												
Pillared zeolite self-pillared organic pillared colloidal suspension	MCM-36 ^{43,44}	101	ITQ-36 ⁵³	69 ^c									
	MWW-BETB ⁶⁵												
		67											

^a Zeolite types are represented by the first material reported and/or by notable examples with references to original reports. Thirteen zeolite framework types, for which at least one of the layered form is known, are reported. References are given for existing layered forms, together with material name. ^b Zeolite layer is common to more than one 3D zeolite framework type. ^c Layered materials obtained by direct synthesis.

Variations in postsynthetic manipulation of LZP materials led to new materials with different 3D arrangement of layers (different interlayer bonding and distances).⁷⁰ The possible postsynthetic modifications of layered zeolite precursors that have been shown in practice are reviewed in Figure 4.

The compilation of known 3D zeolite frameworks is illustrated in Figure 3. It is tempting to propose an alternative system that lists not only the standard 3D zeolite frameworks but also incorporates various 2D forms as well. It could be useful in a number of ways, with better classification and identification being some of the obvious benefits. Recognizing the frameworks as primary structures, the various forms of layered materials are secondary structures, extending the concept of zeolite structures in the second dimension.⁴⁰ The corresponding matrix enables a systematic classification without the need to address the formal problem that many of the 2D forms are not strictly zeolites. The proposed system is presented in Table 1. It provides the name, if available, of the first reported species and/or those materials that are deemed significant for some other reasons.

The MWW zeolite family is again the starting point, providing over 10 distinct secondary structures and additional unique forms identified. Overall, 15 different secondary structures are recognized so far. It is expected that this scheme will expand in both directions and also require revisions and adjustments as the 2D zeolite area grows in the future. It remains to be seen if this approach turns out to be a useful concept adopted for possible general use.

Zeolites and their structures are conveniently and in most cases quite reliably distinguished on the basis of their powder X-ray diffraction (XRD) patterns. It is often the basis for finding atomic coordinates for frameworks; that is, solving the structure. The basic assumption in structural calculations is the treatment of the frameworks as being extended without limits in all directions. The recognition of layered zeolite structures, which are by definition limited in one dimension, begins with the observation that their XRD patterns are similar to but distinct from those of the corresponding complete zeolites. In addition, some XRD patterns change upon calcination or related treatments, as the result of the extra structural flexibility presented by the 2D structure.

As shown by the MWW family, many of its members could be identified and discovered quite reliably on the basis of their XRD patterns. It is possible in many cases to decide by XRD if the attempted preparation procedure was indeed successful. The principles developed for identification of different structures generated by MWW layers should be readily adaptable for other frameworks. A working hypothesis² was proposed that many more, maybe all, zeolite frameworks may show some type of layered form eventually. Similarly, the number of various layered forms may be unlimited.⁴⁰

The original definition of zeolites as 3D entities makes their emergence as 2D materials appear as a contradiction²⁶ or even an oxymoron.²⁷ Two-dimensional zeolites can be viewed as materials where the crystal grows regularly in two dimensions but the growth is constrained in the third dimension. In fact, 3D zeolite frameworks can be viewed, at least conceptually, as a special case of layered structure composed of aligned lamellae that are stacked congruously and fused, producing a covalently bonded 3D framework. The practical illustration of this is the MCM-22P to MCM-22 transformation upon calcinations or the continuous process during crystallization. On the basis of these considerations, we can formulate the relationship between

the two areas of traditional 3D zeolites and the 2D ones in two ways, as illustrated in Figure 5. If only some frameworks can be

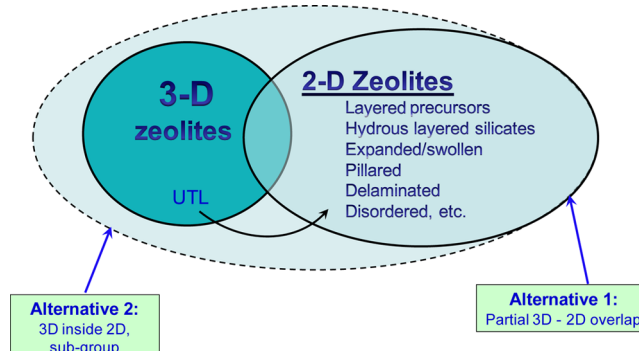


Figure 5. Unified perspective on 3D and 2D zeolites. Two alternatives are proposed: (1) partial overlap between 2D and 3D zeolites and (2) 3D zeolites as a completely encompassed subgroup of 2D zeolite materials.

shown to produce 2D forms, then we have a partial overlap between these two areas. If all frameworks can be viewed as having underlying layered structure, then those with 3D connectivity are a subgroup of the broader 2D area.

4. SYNTHESIS OF LAYERED ZEOLITE PRECURSORS AND OTHER PRIMARY LAMELLAR ZEOLITE FORMS

The definition of layered zeolite precursors described above referred to materials obtained by direct synthesis with layered structure that produced 3D zeolite frameworks upon calcination, or similar treatment, inducing layer condensation. These precursors were aggregates of layers with zeolite-like structure and no covalent bonding between them (see Figure 2). A broader definition must be adopted to account for recent discoveries, for example, a precursor obtained by 3D to 2D transformation.⁷¹ It only requires that layers have potential to produce a zeolite framework (four-connected tetrahedral framework) while they can be synthesized by any means, not necessarily directly. All such materials can be called primary layered zeolite forms and are assumed to be modifiable into various structures.

So far about 5% of known zeolite frameworks have been found to produce 2D forms. As proposed earlier, it may be that many more, possibly all zeolites,² can yield a 2D form in one way or another. In principle, one cannot rule out that any layered zeolite precursor may be eventually available by the standard direct solvothermal synthesis approach. However, at present it is convenient to distinguish three different categories of primary 2D zeolite materials on the basis of synthetic strategy (Figure 6): (1) two-dimensional zeolites obtained by hydrothermal synthesis as layered precursors (MWW family provides a model for that);⁵⁹ (2) surfactant-templated nanosheets, exemplified by MFI;⁷² and (3) precursors obtained by 3D to 2D transformation,⁷¹ that is, disassembly of suitable zeolite represented by the IPC zeolite family derived from zeolite UTL and being part of the ADOR mechanism elaborated below.²³ [Note that ADOR (assembly–disassembly–organization–reassembly) is an acronym for a new mechanism describing synthesis of zeolites starting from an existing zeolite.] These categories are in principle not mutually exclusive, and we envision that layers obtained by one method may be also prepared by the others. Classes 1 and 2 entail direct

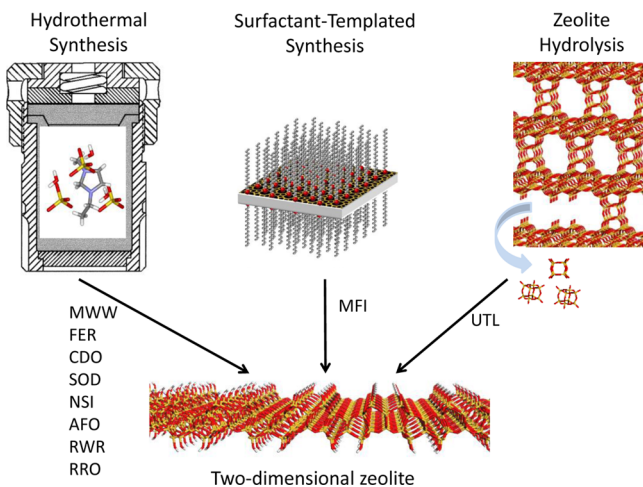


Figure 6. Schematic representation of possible routes leading to two-dimensional zeolites: hydrothermal synthesis, surfactant-templated synthesis, and partial zeolite hydrolysis. Examples of zeolite frameworks for which the two-dimensional analogue has been obtained are also given. Except for surfactant-templated material, the following coloring scheme is adopted: silicon, oxygen, nitrogen, and hydrogen atoms are depicted in yellow, red, blue, and white, respectively.

synthesis like standard zeolites and can be denoted as bottom-up approaches. The 3D to 2D transformation is a two-step top-down procedure but, again, does not preclude future direct synthesis (bottom-up) of similar 2D zeolites.

4.1. Hydrothermal Synthesis of Lamellar Precursors

Layered zeolite precursors (LPZ) and other primary layered zeolite forms are listed in Table 1. The majority of cases are classical layered zeolite precursors, ordered in 3D with expanded interlayer distance that can contract upon calcination to produce a 3D zeolite framework. In addition to these ordered layered forms, there are additional types already mentioned in section 3 for illustrating various possible layer

geometries. Two are obtained with MWW: disordered EMM-10P⁵⁸ and delaminated MCM-56.^{45,59} Figure 7 shows how the different as-synthesized MWW materials are recognized on the basis of X-ray powder diffraction and their structures elucidated. One additional case can be recognized on the basis of materials such as ERS-12.⁷³ It is apparently 3D ordered with template but upon calcination does not produce a complete ordered framework.

The MFI (ZSM-5) framework affords additional layered forms notable for being obtained by direct synthesis: single-layered intergrowth⁷⁴ and self-pillared.⁶⁹ Until shown to the contrary in the future, these two MFI forms do not seem amenable to postsynthetic structural modification and therefore are not strictly zeolite precursors. The MFI obtained by design using a surfactant template is probably not ordered in terms of vertical layer alignment.⁷²

Some zeolites have been obtained only via the layered precursor route: NSI, CDO, RRO, RWR, and PCR. Zeolite NSI is produced by layers that are also found in zeolite CAS: the layers in NSI and CAS are identical but produce two different zeolites due to differences in the symmetry of layer connections.⁷⁵ The former is obtained when layers are propagated by translation, and the latter, by a mirror plane. A similar pattern is also observed for zeolites FER/CDO, RRO/HEU, and FAU/EMT.^{31,76,77}

Zeolite CAS is known but no precursor has been synthesized directly.⁷⁵ CAS layers stacked in the NSI configuration are found in materials denoted EU-19⁷⁸ and NU-6(1), but only NU-6(1) produces zeolite NSI upon calcination.⁷⁹ Surprisingly, EU-19 does not form ordered zeolite NSI upon calcination but forms another material designated EU-20,⁷⁸ with a structure that is still unknown (Figure 8). A special form of the calcined EU-19, designated EU-20b, was reported to contain 88% of the CAS framework based on crystallographic refinement. Its formation is attributed to 180° rotation of every second layer during calcination.⁸⁰ Quantitative modeling and refinement remains to be done. Note that detemplated NU-6(1) and EU-

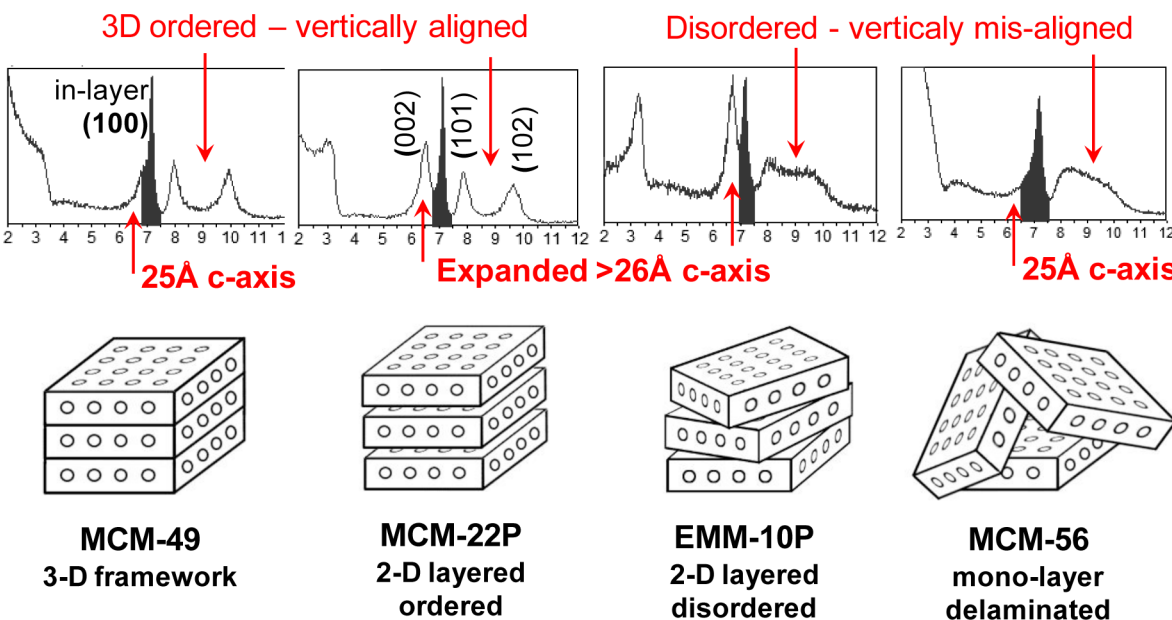


Figure 7. Structures of four distinct MWW materials obtained by direct (one-step) hydrothermal synthesis and their identification based on X-ray powder diffraction features indicated with arrows: for example, lack of separate peak at 6.5° 2θ indicates shorter layer stacking d -spacing (about 25 Å).

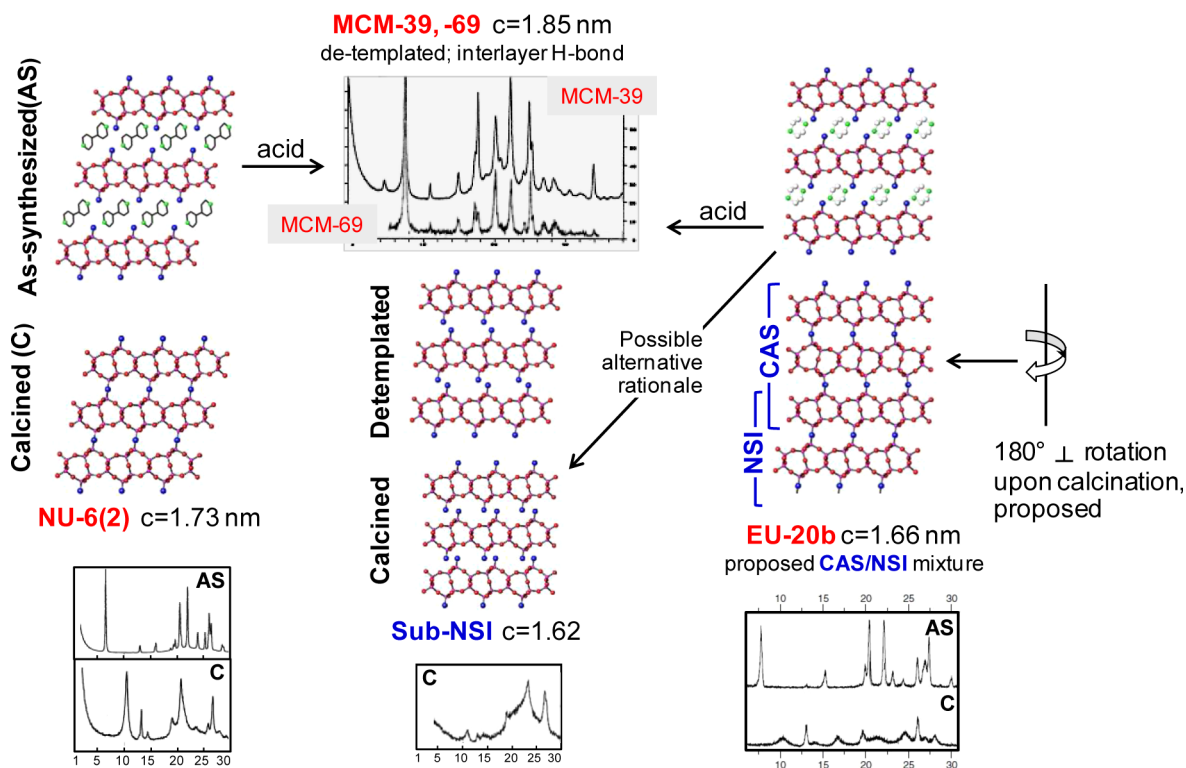


Figure 8. Transformations of NSI layered precursors upon acid treatment and calcination. The proposed CAS framework formation, based on XRD pattern analysis, is supplemented with the alternative sub-NSI formation, which has not been evaluated by calculations.

19,^{78,80} designated MCM-39⁸¹ and MCM-69⁸² have identical, apparently ordered X-ray diffraction patterns, suggesting nothing unusual in the collapse of EU-19.

The other notable cases are those recognized first as 3D zeolites and then also found to exist as layered precursor forms. Here FER and SOD frameworks stand out as well-known, naturally occurring zeolite minerals. This provides basis for the expectation of future discovery of 2D precursors for zeolites now known only in 3D form. In fact it should be noted that lamellar MFI,⁷² discussed in detail below, goes even further by providing a possibly general approach by design to generating zeolite monolayers and their various 2D derivatives.⁸³

Many of the precursors presented in Table 1 have low Al content (and often they do not contain any Al at all) and are considered as a group called hydrous layered silicates (HLS).³¹ They are related to phyllosilicic acids that have been long known and are comprehensively reviewed in the classical treatise on the structural chemistry of silicates⁸⁴ and a recent overview.⁸⁵ They have been thoroughly reviewed in detail in a recent publication discussing many of the points mentioned here.³¹ The reader is referred to the original source for in-depth analysis. An interesting situation is observed with the frameworks FER⁵² and CDO^{86,87} that are made from the same layer,⁷⁵ chosen to be called the ferrierite layer. In FER adjacent layers are related by mirror plane, while in CDO they are related by simple translation. This creates 10–6-ring and 8–8-ring neighboring unidimensional channels. Because the layer has a perpendicular mirror plane, the FER–CDO structural relationship is reduced to a half unit cell shift in the plane of the pore apertures. This conceptual transition has been in fact carried out in practice, starting from CDO precursor converted ultimately to FER zeolite.⁸⁸ This transformation is intriguing from the standpoint of the reverse

direction, that is, FER precursor to CDO, since FER is apparently of lower energy than CDO. Ferrierite layers have been also found as the building units in materials like MCM-47.⁸⁹ They have not resulted in fully ordered frameworks, raising the possibility of being connected to the FER/CDO dualism. Layered precursors PLS-3 and PLS-4, of FER and CDO respectively, were obtained from kanemite as the source of silica.⁹⁰ Zeolite materials ZSM-52 and ZSM-55 were reported in the late 1980s, well before MCM-22, but were only recognized as CDO precursors much later.⁸⁷ They may be of interest as possibly carrying Al and B centers and because they are made with the inexpensive template choline.

One of the HLS materials, RUB-18,^{91,92} undergoes a unique transformation into the zeolite framework RUB-24 (designated RWR)⁹³ with formation of 8-ring channels. The corresponding axial dimension changes from 4.4 nm in Na-RUB-18 to 2.73 nm in RUB-24. Interestingly the ordered RUB-24 structure is not obtained by direct condensation from the original Na-RUB-18 but after intercalation with organic tetramethylammonium cation. This is an example of an organic SDA organizing precursor layers to yield an ordered structure. This phenomenon is presented below as playing a decisive role in synthesis of the new zeolite PCR by the ADOR strategy.²³

So far only one aluminophosphate, AFO (AlPO-41), is represented among layered zeolite precursors. AFO was obtained both directly⁹⁴ and from the layered aluminophosphate precursor templated by a bulky macrocyclic polyamine as the structure-directing agent.⁹⁵ The complete AFO topology required translation of alternate layers by half a unit cell in both *a* and *b* directions, followed by condensation. It is reasonable to expect that more AlPO-type materials will be found to have a layered precursor. No fundamental reason preventing that is imagined at this time,⁹⁶ but it remains to be seen.

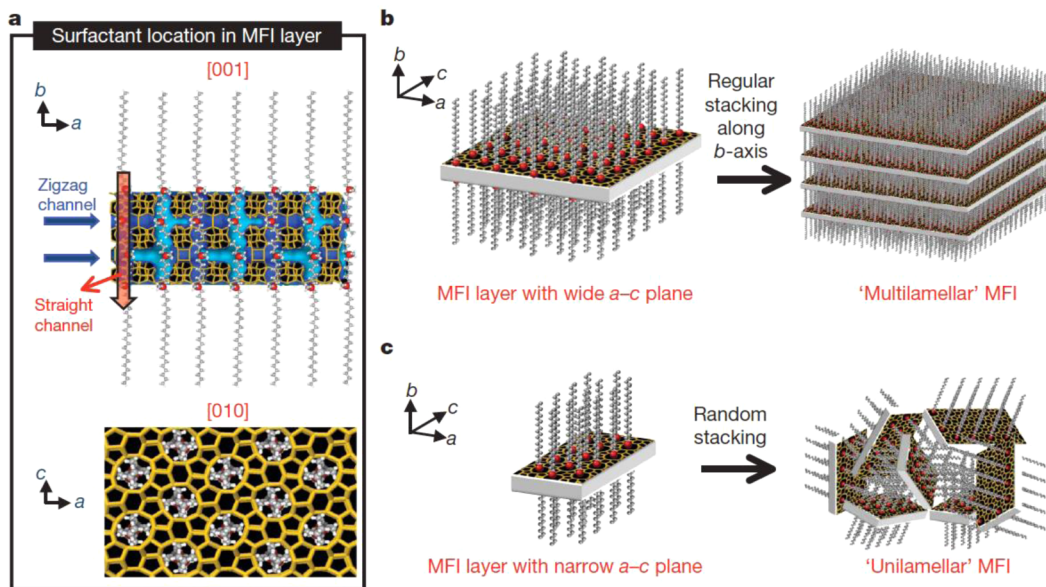


Figure 9. Use of a surfactant with a cationic headgroup that can direct the MFI structure to nanosheets with approximately 1 and 0.5 unit cell thickness. These nanosheets can either stack in an ordered fashion or be randomly stacked to form different types of material. Reprinted with permission from ref 72. Copyright 2009 Nature Publishing Group.

The framework MWW produces a variety of 2D zeolite structures, directly and by postsynthetic modification, giving rise to the family of MW/MCM-22 materials, which is most abundant and diverse. It is a model by providing a majority of the first examples of new 2D structure types. Many still remain unique, although in principle there is no fundamental reason preventing other frameworks from yielding such architectures. Particularly notable is the formation of four different materials by direct synthesis:⁵⁸ the complete 3D framework (MCM-49); the layered precursors, ordered (MCM-22P) and disordered (EMM-10P and related species); and delaminated (MCM-56), as shown in Figure 7. As the leading 2D zeolite family, the MW (MCM-22) materials have been thoroughly reviewed in great detail,^{2,58} and herein only the highlights will be mentioned. The family is a case study for the application of X-ray crystallography as the primary tool for recognizing and distinguishing various layer arrangements, that is, different 2D structure types. The MCM-22 unit cell turned out fortuitously to be particularly suitable for such analysis because of its hexagonal³⁰ rather than monoclinic or triclinic unit cell. This guarantees invariance of intralayer ($hk0$) peak positions as the interlayer distances and orientations change. Furthermore, conveniently the complete set of all diagnostic reflections, comprising representatives of the intralayer ($hk0$), interlayer ($00k$), and cross-layer zones ($h0l$), is found in a narrow $6\text{--}10^\circ$ 2θ range (Cu $\text{K}\alpha$ radiation). Detailed analysis of the correlation between XRD pattern and structure is available elsewhere.⁴⁰

4.2. Surfactant-Assisted Synthesis of Nanosheet Zeolites

Perhaps one of the most interesting and important discoveries in zeolite science has been the use of organic templates during synthesis to direct the structures of new zeolites.^{97,98} Since the very early descriptions of zeolite synthesis using organic additives, the majority of new zeolite materials have been prepared this way. The general concept is very simple: cationic organic molecules balance the charge of the framework and/or they fill space in the voids, thus stabilizing the formation of zeolites under the required conditions. Normally the organic cations used are relatively small or medium-size, with a limiting

charge density that controls how they interact with the charge on the zeolite framework. In the 1990s, researchers at Mobil discovered that surfactants can also direct silicate and silica structures,⁹⁹ but this time through a liquid crystal mechanism that eventually leads to so-called ordered mesoporous solids,¹⁰⁰ materials with larger pore sizes than zeolites (up to hundreds of nanometers pore size) but with walls having less structural order.

Surfactants are molecules that have two distinct chemistries: a hydrophilic headgroup, which is often charged, and a hydrophobic tail. Ryoo and co-workers⁷² made the important link between the structure of the usual organic templates used for zeolite synthesis and that of certain surfactant head groups: the head group of the surfactant could act to template a zeolite structure and the tail would not allow zeolite crystal growth along that direction, potentially leading to directly grown two-dimensional zeolites. Ryoo's work has been spectacularly successful and has resulted in several families of new hierarchical zeolites.^{72,101,102} In the original work, the surfactant $\text{C}_{22}\text{H}_{45}\text{-N}^+(\text{CH}_3)_2\text{-C}_6\text{H}_{12}\text{-N}^+(\text{CH}_3)_2\text{-C}_6\text{H}_{13}$ with a long alkyl chain was designed so that the dicationic headgroup would be a suitable structure-directing agent for the synthesis of a zeolite with the MFI structure. Recently, this approach was successfully applied also for synthesis of layered aluminophosphates.¹⁰³ However, the tail group effectively blocks zeolite crystal growth in one of the three possible directions, leading to zeolitic materials that are zeolite sheets of only 2 nm thickness, equivalent to only one unit cell (Figure 9). Ultrathin zeolites of this kind have two great advantages. First, they have a large number of accessible catalytic sites on the external surface of the zeolitic nanosheets, and second, diffusion limitations are reduced, which has benefits in both increasing activity and reducing coke deposition, leading to long-lifetime catalysts, for example, for the methanol to gasoline (MTG) conversion.⁷² Depending on the synthetic conditions and modification of template structure, the authors could control the final morphology of the nanosheet zeolites, from ordered stacking of the nanosheets on the one hand to unilamellar arrangements

with no stacking order whatsoever (Figure 9). In extensions on the work, Ryoo and co-workers¹⁰¹ have shown that the nanosheets can be pillared by use of silica to produce materials with a hierarchical porous system.

A beautiful example of the control possible in this work is that changing the number of quaternary ammonium species in the surfactant from two (as described above) to three and four leads to nanosheets of different thickness: the more cationic units in the surfactant head groups, the thicker the zeolite nanosheet.^{83,104} Such precise control over crystallite morphology is an important feature in our goal of designing new materials for specific purposes. In addition, the precise control of layer thickness at this dimension level is exciting for the preparation of other zeolitic materials.

A recent report claimed one-pot structural conversion of magadiite into MFI zeolite nanosheets by use of monoquaternary surfactants as structure and shape-directing agents.¹⁰⁵ The most likely pathway is recrystallization producing standard, possibly platelike MFI crystals. One piece of evidence suggesting this is the much lower intensity of the interlayer (001) reflections with *d*-spacing of 5–6 nm than reported in the studies by Ryoo and co-workers.¹⁰¹

4.3. Two-Dimensional Zeolites Synthesized on Metal Supports

An alternative type of 2D zeolites is those supported on metal surfaces. They are not strictly the same as the free-standing 2D zeolites described above but they are of sufficient similarity to warrant discussion, especially with regard to computer simulation methods. Well-defined aluminosilicate thin films were first prepared on a Mo(112) substrate.¹⁰⁶ The structure was assigned on the basis of good agreement between calculated and experimental characteristics. The monolayer thick film is composed of (SiO_4) and (AlO_3) units strongly bound to the support by Si–O–Mo linkages, and it does not possess a negative framework charge, contrary to zeolites. A completely different interaction between the silica film and metal support was reported for a silica bilayer formed on the Ru(0001) surface, where the interlayer interaction was dominated by the dispersion and electrostatic forces.¹⁰⁷ An aluminosilicate thin film weakly bound to the support was reported only recently.¹⁰⁸ This aluminosilicate film possesses a framework negative charge, and thus it exhibits Brønsted acidity. It can be considered as a special case of a 2D zeolite quite relevant for this review, and it is therefore discussed below in greater detail.

4.4. Three- to Two-Dimensional Transformation of Parent Zeolites

All the examples of synthesis of 2D zeolites described above represent the bottom-up preparation, usually by hydrothermal synthetic methodology. An alternative concept is the top-down approach, where a 3D framework is selectively disassembled into a 2D layered material. Since all T–O bonds in a zeolite are essentially equivalent, at first glance this might seem like a very difficult thing to do. However, engineering weakness specifically into certain areas of zeolite structures is an area that has developed significantly very recently. Much of this work is built on the recognition that incorporation of germanium into zeolites tends to promote certain secondary building units, especially the double four ring (D4R).¹⁰⁹ Added to this is the fact that Ge is significantly more reactive than Si in many ways; it is especially sensitive toward hydrolysis.

The utilization of germanium in zeolite synthesis has certainly been recognized as a method of producing novel topologies in recent years.^{109–111} Several new materials have been prepared with some remarkable structures, including solids with large pores and unusual secondary building units such as double three rings (D3R).³⁵ More recently, it also became apparent that Ge is very unusual in being incorporated remarkably selectively into certain units, so much so that it is has been suggested as a major structure-directing factor in favoring materials that contain D4R units.^{112–114} However, despite the great interest in the topologies, new applications have been less forthcoming for Ge zeolites. A major reason for this is the rather low hydrothermal stability of the materials. The reason for the low stability is the rather higher reactivity of the germanium toward water, and this was recognized by several researchers as a potential opportunity for manipulating the properties of the zeolites via selective hydrolytic removal of germanium.^{115,116} Several groups have shown that Ge can be removed from germanosilicate frameworks, either being replaced by other atoms, like aluminum,¹¹⁷ or to produce new zeolite topologies by removing the germanium followed by a thermal calcination to provide an inverse sigma transformation route to new topologies.²²

Other researchers noted that if there is enough Ge in the material, there is the opportunity to remove completely the D4R units, leaving behind layered 2D zeolites.⁷¹ These layers can then be manipulated in the same manner as the directly synthesized 2D zeolites described above.^{23,70} The strategy behind this process is shown in Figure 10.

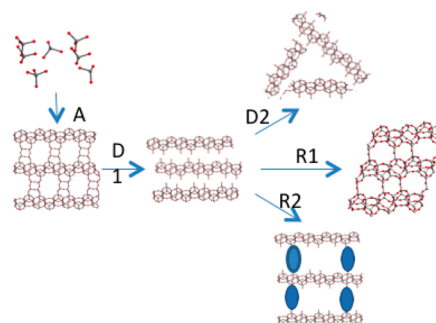


Figure 10. Selective removal of Ge from the UTL structure leads to layered materials, for example, IPC-1P, that can be manipulated into different materials through hydrolysis or reassembly in various different ways.

4.5. Assembly–Disassembly–Organization–Reassembly Strategy

Perhaps the most interesting property of the 2D zeolites prepared in this fashion is that because they are derived from fully connected zeolites, they are geometrically suitable for the reassembly of the layers into fully connected zeolite topologies. This is not necessarily the case for other 2D zeolites assembled from small fragments by hydrothermal synthesis and having template molecules between the individual layers. This leads directly to the so-called ADOR (assembly–disassembly–organization–reassembly) strategy, where fully connected zeolites can be prepared by taking advantage of the geometrically restricted 2D layers. Figure 11 shows the strategy behind this process where the Ge has been removed in a chemically selective way from the UTL structure. The resultant layers have

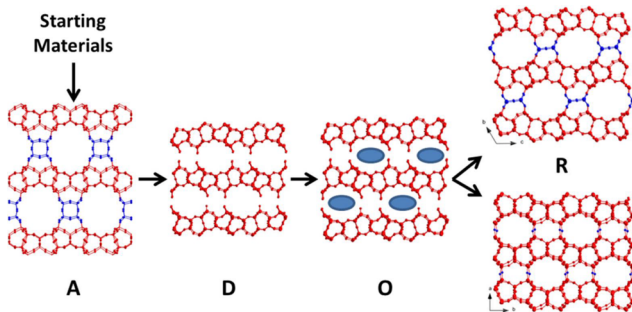


Figure 11. ADOR strategy for the preparation of zeolites. Stage A is the assembly of a zeolite from the starting materials; D is the controlled disassembly of the zeolite; O is an organization step whereby a new linking unit or a structure-directing agent (blue oval) is incorporated; and R is the final reassembly step. In the case of zeolites IPC-2 (OKO) and IPC-4 (PCR), there is no direct synthesis route yet available. The color key is as for Figure 1, with the layers common to all materials shown in red and the different linkers shown in blue.

been linked in two different ways to produce a family of zeolite structures with PCR and OKO topologies.^{22,23}

A particularly attractive feature of the ADOR process is that while Ge is selectively incorporated between the layers of the starting UTL structure, other elements are not incorporated in the same way.^{114,118} This means that, for example, aluminum is incorporated into the layers and is therefore preserved through the whole process. As a result, the catalytic sites in UTL are still present in the PCR material, making this process amenable for the production of functional solids. Importantly, isomorphous substitution of B, Al, Fe, and Ga into the UTL framework has been evidenced, strengthening the catalytic potential of this new family of zeolites and zeolite-related materials.^{119–121}

The critical issue in this 3D to 2D transformation, as well as in the subsequent condensation, is proof of preservation of the structural integrity of UTL layers.⁷⁰ It seems that this is not always the case, as some other authors reported 3D to 2D transformation of MWW to MCM-22P in the presence of an appropriate organic template. In that case it may be suggested that a solution-mediated recrystallization mechanism is probably operative.¹²² In a similar way, the integrity of the original layered material should be proven, when a zeolite such as MFI is produced from the layered silicate.¹⁰⁵

It is believed that the ADOR mechanism can operate also for other germanosilicates having D4R or D3R rings connecting zeolitic layers. Critical factors of this operation are high concentration of Ge in the structure (D4R or D3R rings) and geometrical suitability of layers to be condensed together.

A recent theoretical study by Treacy and co-workers¹²³ predicted that there are many possible low-energy zeolite structures based on the double-layered structure that has recently been noted as present in several known zeolite materials. This offers further opportunities to think about how new zeolites with different pore sizes could be prepared by use of layered zeolite materials as building blocks.

5. POSTSYNTHETIC MODIFICATION OF LAYERED ZEOLITE PRECURSORS

The most significant practical feature of layered zeolite precursors is their structural flexibility. There are no interlayer covalent bonds in LZP, and the interlayer distance, orientation, and bonding can be modified all the way to being completely separated into individual sheets. One can imagine any

geometric configuration as eventually possible, although in practice it is prudent to limit oneself to some well-defined distinct layer arrangements as ultimate goals for synthesis, characterization, and practical use. Recently, MFI has contributed some unprecedented lamellar structures like single-layered intergrowths and self-pillared materials (section 4.2).^{69,74}

It is convenient to discuss a particular modification of layered zeolite for MWW materials first. Postsynthetic modifications that attract the most attention are those resulting in expanded and more open layered structures as well as those that can be still further modified. The expanded ones are perceived to offer enhanced catalytic capability for activating larger molecules that are not processed by standard frameworks. The synthetic pathways and characteristics of products will be presented in detail, but we begin with a seemingly trivial modification: detemplation.

5.1. Precursor Detemplation

The formation of many layered precursors is attributed to particular organic SDA molecules, which apparently become attached to the flat layer, line the surface, and prevent attachment of another layer with formation of T–O–T bridges; that is, they stop propagation of complete framework in the third dimension. They work in the same manner as designed templates for synthesis of MFI nanosheets by Ryoo and co-workers.⁸³ There is often extensive hydrogen bonding between SDA molecules and silanol groups on the layer surface.^{78,79} The crystals comprising the precursor consist of alternating layers of SDA and zeolite. Even in the case of MCM-22P, where a particular type of hydrogen bonding between silanols was proposed,¹²⁴ a strong influence of the template (hexamethylenimine) trapped between layers seems to play a significant role. This role is not fully elucidated but may even be crucial in producing MCM-22P as an ordered material during crystallization. The SDA molecules are usually tightly bound but can be extracted by appropriate treatment, for example, with an acid. This is typically accompanied by contraction of the interlayer distance. The representative values are 0.2 nm for MCM-22P and even up to 3–4 nm for MFI. In the case of NSI zeolite precursor NU-6(1), detemplation was cited as crucial for efficient expansion of the interlayer separation, swelling, and subsequent pillaring.⁸¹ Another example of beneficial detemplation effect occurs with the SOD precursor RUB-15.¹²⁵ While calcination of the as-synthesized material produced a poorly defined product,¹²⁶ upon treatment with acetic acid followed by calcination, an ordered SOD framework was produced.^{125,127}

In the case of MCM-22P, the treatment with acid solution induces 0.2 nm contraction, as seen upon calcination, but simultaneously lateral disorder is introduced. This is observed in X-ray diffraction, showing a pattern similar to delaminated MCM-56, discussed in detail below. Specifically, the interlayer peaks initially present in MCM-22P, (101) and (102), form after treatment a single broad band indicating disorder. The product is referred to as an MCM-56 analogue (not MCM-56 itself)^{60,61,128} because it may retain the interlayer connection between silanols, which is assumed to be absent in MCM-56 (Figure 7). Whether this is indeed the case remains to be determined. MCM-22 samples and the MCM-56 analogues obtained by treatment with 0.1 M HNO₃ were compared side-by-side by various methods including catalytic testing.¹²⁹ The X-ray diffraction of MCM-22P became similar to MCM-56

upon this treatment. The calcined MCM-56 analogue showed broadened ²⁹Si and Al NMR maxima, but they were otherwise qualitatively similar. The overall Brunauer–Emmett–Teller (BET) surface area decreased from 476 to 415 m²/g, but the external surface increased (118 to 145 m²/g). This was rationalized as the MCM-56 analogue having more edges of the structure exposed to the outside, thus presenting partially delaminated structure. In liquid-phase benzene alkylation with ethylene, the MCM-56 analogue gave a higher yield of ethylated benzenes and better resistance to deactivation than the corresponding MCM-22 sample. The presented data did not indicate the preservation or severance of interlayer bonding as a result of the acid treatment. This leaves the equivalence between MCM-56 itself and the MCM-56 analogue unresolved.

In the formal sense, the material designated IPC-1P, obtained from UTL by a 3D to 2D transformation as part of the ADOR strategy and discussed in detail in section 4.5, may be viewed as a detemplated precursor.⁷¹ It has a relatively well-defined structure because of apparent extensive hydrogen interlayer bonding.¹³⁰

Calcination of detemplated precursors may lead to disordered layers deduced from broad and weak intensity X-ray peaks.⁸¹ Such products may also exhibit interlayer *d*-spacing that is shorter than in the corresponding condensed zeolite. This may be explained by vertical mismatch between opposing silanol groups and their submerging into a surface trough. The name suggested for such materials is subzeolite (e.g., sub-NSI).⁸¹

Another example of the above behavior is found with Na-RUB-18. It readily exchanges Na for protons in diluted acids.¹³¹ The product H-RUB-18 is crystalline but with considerable distortion (of the layers) and high degree of structural disorder. It was reported in two forms, α and β , with axial lengths 2.976 and 2.6 nm.

5.2. Expansion of Interlamellar Space

The breaking of interlayer bonds and expansion of interlamellar space is a critical process enabling subsequent modifications of layered solids. It is often called swelling and has been well developed with clays, phyllosilicates, and layered metal oxides.^{56,132–134} Zeolite precursors initially required quite severe and innovative approaches to achieve complete swelling. MCM-22P yielded the first swollen precursor, which was not the final goal but an intermediate step toward the pillared zeolite MCM-36.⁴³ Swelling of MCM-22 was later applied as the first step to synthesize the delaminated ITQ-2 (Figure 2).⁶⁶ The initial swelling procedure was quite severe,⁴³ and subsequently milder variations were reported.¹³⁵ The particular requirements were high concentration of surfactant and hydroxide (OH^-) ions combined with elevated temperature. High pH had to be balanced to minimize the possibility of dissolving the parent materials with the possible consequence of the formation of siliceous mesoporous phases¹³⁶ that were recognized as new materials.¹³⁷ There was also an additional condition for swelling, namely, the absence of cations that could compete with the surfactant by interacting preferentially with the precursor, which would preclude cationic surfactant molecules from producing the swelling. The nature of this detrimental cation influence was uncertain but was initially attributed to cation size.¹²⁴ Small cations were believed to migrate into the interlayer region in MCM-22P and hinder swelling. Tetrapropylammonium hydroxide (TPA-OH) proved later to provide the needed hydroxide ions without obstruction

of swelling. The original successful swelling of MCM-22P was achieved with cationic surfactant in the hydroxide form generated by partial anion exchange. Later, a more convenient surfactant halide/TPA-OH mixture was also found to be effective. In this first case of zeolite precursor swelling, the proper characterization of the product and confirmation of its desired nature was of crucial importance. The ultimate evidence was obtained by characterization of the pillared sample as described in section 5.4, but initial X-ray diffraction pattern of the swollen product was also of great value. Two novel features in addition to the expected changes in some peak positions were obtained. The first was a low-angle peak >5 nm *d*-spacing due to expanded interlayer space and absence of the peak at ca. 1.35 nm [(002) reflection of MCM-22P], signifying complete transformation of the original MCM-22P. Simultaneously, prominent diffraction lines corresponding to intralayer reflections with $(hk0)$ indices remained in their original positions indicating preservation of MWW layers, more or less quantitatively. The new features included a peak at ca. 1.6 nm ($5.5^\circ 2\theta$), initially unassigned, and a broad band in the range 8 – $10^\circ 2\theta$. The former was later attributed to the (003) reflection.¹³⁵ As for the broad band between 8 and $10^\circ 2\theta$, it indicated disappearance of atomic order in the third dimension, which in the original MCM-22P is shown by two separate interlayer peaks in this 2θ region. This provided a semi-quantitative measure of the efficiency of swelling, which could be judged successful based on the presence of separated maxima in the range 8 – $10^\circ 2\theta$.¹³⁸ The absence of the latter and the depth of the resulting “dip” were indicative of incomplete swelling and its degree. This broad band proved to be a crucial indicator because another complication was identified during this original study, namely, the possibility of surfactant-assisted formation of mesoporous phases like MCM-41 or more generally M41S.¹³⁹ In fact, this was one of the routes that led to discovery of Mobil’s mesoporous materials.¹³⁷ One of the transmission electron microscopic (TEM) images that revealed the hexagonal structure of MCM-41 also shows a cross-section of MCM-22P as evidence of unsuccessful swelling despite an apparent low-angle line in the XRD pattern. The “danger” of unwanted formation of mesoporous contaminants was also mentioned in connection with sonication to make ITQ-2 at temperatures above 50 °C.¹⁴⁰ It is not expected that sonication alone would cause formation of MCM-41, as it is more likely to begin during swelling that is carried out at 100 °C. The formation of M41S-type mesoporous solids during swelling may be detected by calcination of some part of the product and characterization by X-ray diffraction and adsorption. Even the lamellar MCM-50 retains significant porosity despite structural collapse and may contribute to ultimate high BET surface area of putative pillared/delaminated zeolite.¹⁴¹ Such control and precautions are strongly recommended, especially when modifying a new zeolite system for the first time. Proper swelling is crucial for pillaring, which as far as we know is quite routine when carried out with tetraethyl orthosilicate (TEOS) and when excessive moisture is avoided.

The severe conditions of MCM-22P swelling were subsequently revisited and explored under less drastic regimes. In particular, the surfactant/TPA-OH was used at room temperature and enabled a high degree of swelling with less damage to MWW layers.¹³⁵ It was also shown that the intercalated surfactant can be removed by treatment with acid in alcohol, resulting in recovery of the layered precursor. Subsequent studies revealed that the question of optimal

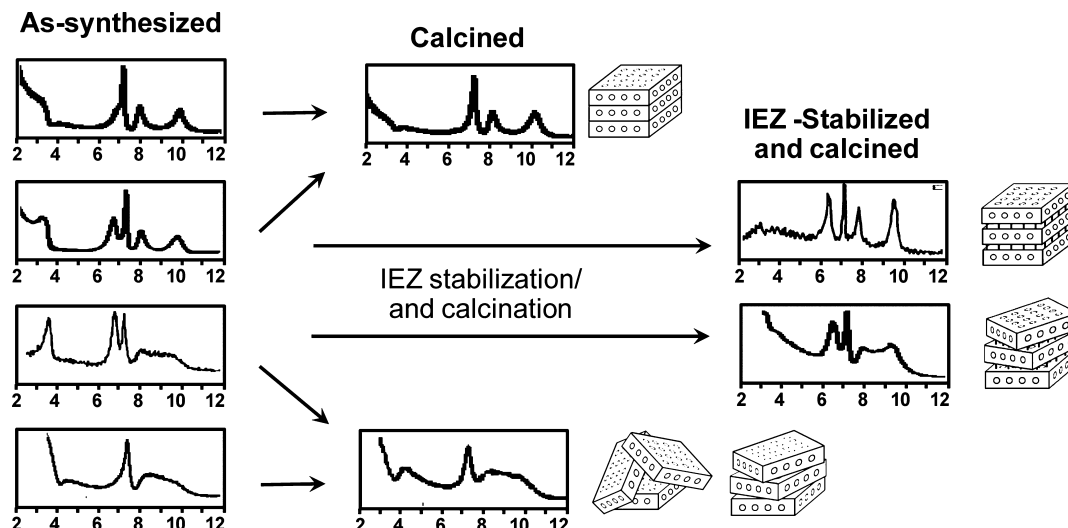


Figure 12. XRD patterns of MWW structures showing four different as-synthesized materials producing only two different patterns upon calcination and an additional two (“missing”) types that can be obtained upon stabilization, matching the “as-synthesized” set of four distinct X-ray pattern profiles.

MCM-22P swelling may be far from over.¹⁴² The qualitative trends showed that increasing Al content in the precursor or lowering amount of the hydroxide may cause incomplete swelling as judged from the XRD pattern, especially based on the mentioned diagnostic dip in the 8–10° region. It was also observed that the use of TMA-OH (tetramethylammonium hydroxide), which has a smaller cation size than TPA-OH, as the source of base was surprisingly effective to a significant degree, although swelling was not complete.¹⁴³ It was unexpected as it undermined the previous rationale for the effect of cation size upon swelling of MCM-22P.¹²⁴ There is also a renewed interest in the use of the surfactant hydroxide (CTMA-OH, cetyltrimethylammonium hydroxide) as the swelling medium. It shows close to maximum efficiency based on XRD of the products, which may be due to high hydroxide concentration. The application of CTMA-OH entails additional cost and labor (the need for anion exchange), which makes it less convenient to use, but one cannot rule out its preferred status if the reagent is available commercially.

The use of a high-pH medium for swelling can be viewed as similar to production of hierarchical zeolites through desilication. The decrease in Si/Al in swollen MCM-22P can sometimes be quite significant^{144,145} and may entail beneficial desilication effects. This perspective has so far not been considered explicitly in detail.

Wang et al.¹⁴⁶ studied the effects of amount of swelling agent (CTMA-Br and TPA-OH), pH of the synthesis system, and Si/Al ratio of MCM-22P on the swelling efficiency and synthesis of ITQ-2 zeolite. They concluded that “well-swollen MCM-22P could be obtained within only 4 h at pH = 11.5 by decreasing the amount of swelling agents”. This is outside the range of conditions believed to be required. The positive outcomes cited included decreased desilication, significant increase in the ITQ-2 zeolite yield, “the ultrasonic exfoliation process became more accessible”, and the “MCM-41 mesophase could be avoided due to lower pH value”. Furthermore, the reported facile delamination at lower Al content was rationalized as follows: the “higher the Si/Al ratio of the MCM-22(P), the lower the charge density on the sheet surface, the weaker the electrostatic attractive force and the intermolecular force between the

interlayer cation and negatively charged sheets, which made the intercalation, swelling and ultrasonic exfoliation easier”.

The swelling procedures developed for MCM-22P were also applied, apparently successfully, for layered precursors of other zeolites. Precursors of NSI (MCM-39)⁸¹ and PCR (IPC-1P)⁷⁰ were reported to swell readily in detemplated forms and then were treated with TEOS to afford pillared derivatives.

In separate studies, the precursors NU-6(1) (NSI)¹⁴⁷ and PREFER (FER)⁵³ were treated with alkyltrimethylammonium hydroxide at pH = 12 and cetyltrimethylammonium bromide/TPA-OH mixture, respectively, with the original template between the layers. The products were subjected to pillaring and delamination, to be discussed in sections 5.4 and 6. An alternative approach to high-pH treatment of layered precursors was tried for breaking the interlayer MCM-22P bonds and delamination, and is also presented in section 6.1.¹⁴⁸

While the expansion/swelling of zeolite precursors is typically attempted in a high-pH environment, the layered silicate RUB-18, which affords zeolite RWR, was investigated at conditions close to neutral. It should be noted that RUB-18 is considered isomorphous with silicate materials known as ilerite¹⁴⁹ and octosilicate, which have been studied for their intercalation, pillaring,¹⁵⁰ and surface modification¹⁵¹ capabilities. This view from the layered zeolite versus hydrous layered silicate perspective should make no difference in actual chemistry. Nonetheless, it seems that so far RUB-18/ilerite/octosilicate could be modified quite easily.^{152,153} At the same time, differences are observed in comparison to precursors swelled at high pH. For example, Na-RUB-18 intercalated with cetyltrimethylammonium cation by exchange is expanded by 1.7 nm,¹⁵² while MCM-22P and IPC-1P are expanded by over 2.5 nm.

5.3. Stabilizing Interlayer Expanded Precursors

Multilayered zeolite precursors are usually obtained with the organic SDA in the interlayer space, which somewhat expands the layer spacing in the stacking direction. Calcination eliminates these SDA molecules from the structure, with concomitant contraction and condensation producing 3D frameworks. Depending on the conditions and type of SDA, the condensation can provide more or less well-ordered

materials. For the expansion of interlayer space described above to be permanent, some kind of propping with thermally stable moieties or pillars is required. Stabilization refers to a process that enables as-synthesized precursor to preserve its expanded form upon calcination, showing increased basal spacing compared to the corresponding conventional zeolite, for example, by 0.23 to 0.27 nm for MWW.⁶³ This occurs when appropriate thermally stable bridging groups, such as SiR₂ where R = alkyl or OH, become incorporated between the layers. The products are called interlayer expanded zeolites (IEZ) and resemble the parent zeolites but have enlarged pore openings between the layers. For example, the stabilized zeolite MWW, IEZ-MWW, has a 12-ring opening compared to a 10-ring one in the conventional zeolite.¹⁵⁴ The corresponding basal *d*-spacing (*c*-unit cell) is equal to 2.7 nm rather than the 2.5 nm found in MCM-22, which is slightly larger than in MCM-22P.^{62,154} Except for a special case, like the IPC-2 material, these stabilized precursors are not strictly zeolites due to the lack of four O–Si or equivalent neighbors around the bridging Si moiety. The remarkable thing with the stabilized precursors is that they can be viewed as the first and unique examples of pillared layered structures with ordered pillars. The stabilization of precursors manifests an interesting pattern in the context of the four different MWW species already discussed to form by direct synthesis (Figure 12). Upon calcination, these four materials (MCM-49, MCM-22P, EMM-10P, and MCM-56) produce only two distinct XRD patterns as the expanded structures (MCM-22P and EMM-10P) collapse. Stabilization prevents contraction upon calcination and the “missing” patterns (on the right) are indeed possible in the calcined forms as well.

The discovery of the stabilized (IEZ) form of layered zeolites was unexpected and happened after the standard types of modifications—swelling, pillaring, and delamination—seemed to have exhausted the list of principal options for structural modification of LZPs.⁵⁹ The unexpected stabilization was discovered when a Ti-MWW layered precursor was heated in strong acid medium.⁶² In this process, silicon atoms with OH attached (geminal silanols) became inserted selectively between opposing Si–O groups on the surface. The product, designated Ti-YNU-1, had interlayer *d*-spacing after calcination of around 2.7 nm, similar to the precursor. The authors mentioned⁶³ that this first case “has been obtained only by chance when a postsynthesized Ti-containing MWW precursor with an extremely low Ti content was acid-treated”.^{62,154} The effectiveness of this new process was attributed to the presence of some soluble or dissolved silica that can be inserted as monatomic bridges between the layers. Subsequently an alternative approach to such stabilization was developed.⁶³ It entails deliberate use of silylating agents, usually alkoxy silanes such as dimethyldiethoxysilane, and was initially demonstrated with stabilized zeolite materials MWW, CDO, and FER.⁶³ This report also included MCM-47, which is similar to FER and CDO in having the same FER layers but its calcined structure is not fully elucidated and probably disordered.⁸⁹ IEZ forms were also generated by alkoxy silylation with RUB-39,¹⁵⁵ precursor of RWR; RUB-51, the precursor to the framework SOD;¹⁵⁶ and the layered precursor IPC-1P, discussed separately. Stabilized CDO (APZ-1 and -3; atomic pillared zeolite) and FER (APZ-2 and -4) materials were also produced by acid treatment with 1 M HCl without addition of alkoxy silylating reagents.¹⁵⁷ The PLS-4 material, which is a CDO precursor, was stabilized both by acid-only treatment and by alkoxy silylation.¹⁵⁸ In both cases

the stabilized product was obtained, but the latter treatment gives a more extensive stabilization as judged from the BET area of the products.

The initial bridging moiety obtained upon alkoxy silylation may be written as (layer-Si)-O-Si(CH₃)₂-O-(Si-layer). Upon calcination, the methyl groups are oxidized to OH, producing Si(OH)₂ moiety between layers. The presence of the dimethylsilyl and geminal silanols has been confirmed by NMR and IR spectroscopy. When two Si(OH)₂ groups are close enough, they can condense as shown with IEZ-FER.¹⁵⁹ A remarkable situation happens with IPC-1P (section 4.3). The bridging groups form a square between the layers and are close enough to condense into a fully connected zeolite framework (IPC-2 isomorphous with OKO).^{22,23}

The preparation of IEZ materials is quite facile and highly efficient with precursors having high Si/Al or Si/Ti ratio, which is the case with most known layered zeolite precursors. MWW is an exception because it affords precursors with a wide range of Si/heteroatom ratios down to Si/Al = 10–15. The increasing content of Ti from Si/Ti = 100/1 to 30/1 in MWW decreased the effectiveness of precursor stabilization.¹⁶⁰ The stabilized Ti-YNU-1 structure was absent, and no IEZ-MWW formed starting from Si/Ti = 50 down.

IEZ-MWW with Al presents a different problem, the leaching of Al from the framework in the strongly acidic medium used for silylation.¹⁶¹ Various conditions were tested for Al-MWW with Si/Al in the range 28–35.¹⁶² A basic environment (NH₃, NaOH) and alkoxy silanes with more than two alkoxide groups did not result in stabilization upon 24 h reaction under reflux. The high retention of Al in tetrahedral sites was obtained by a two-step approach. Al-MWW was first treated with 0.1 M HNO₃ and then silylated in 1 M NH₃ or in water. Another approach relied on vapor-phase silylation of Al-MWW precursor (Si/Al = 33) with SiMe₂Cl₂ followed by calcination. The obtained IEZ-MWW showed strong acidity similar to that found in 3D zeolites.¹⁶³

5.4. Pillaring

Pillaring is a more general and older concept than stabilization. Pillaring of layered precursors is based on the idea of converting dense, layered metal oxides and silicates into high-surface-area molecular sieves with large interlayer separations.¹⁶⁴ The “pillars” are typically amorphous and not arranged in an ordered fashion, in contrast to the above stabilized products with ordered props. In comparison to previously studied 2D solids, exemplified by clays, the layered zeolite precursors provided a step change rather than an incremental catalytic opportunity by offering in principle unprecedented benefit of strong acid sites in the layer. Indeed, the first example of pillared zeolite, obtained from the MWW precursor MCM-22P and denoted MCM-36, was a hybrid with micro- and mesopores and zeolite acid activity⁴³ leading to outstanding catalytic performance.⁶⁸ Pillaring of layered materials had been known and practiced since at least the 1970s,⁵⁵ which could be achieved by simple ion exchange with clays. For the dense oxides mentioned above as well as zeolite precursors, the requirements were more demanding. So far, swelling with surfactants is the prerequisite and complete separation of the layers plays a critical role. Pillaring is accomplished by absorption of “pillar precursor such as tetraethylorthosilicate (TEOS) into the organophilic interlayer region, where it is converted to a metal oxide pillar”.¹⁶⁴ The final material is produced by calcination for several hours in air at 538 °C,

which removes the water, preswollen organoammonium ions, and organic byproducts from TEOS hydrolysis, affording a silica-pillared product.¹⁶⁴ In some cases, the TEOS-treated materials are contacted with water to hydrolyze the intercalated silica precursor before calcination.

Pillared zeolite derivatives were reported for the following topologies: MWW (MCM-36),⁴³ FER (ITQ-36),⁵³ NSI [MCM-39(Si)],⁸¹ MFI,¹⁰¹ ilerite,¹⁵⁴ and PCR.⁷⁰ The transformation of a layered precursor like MCM-22P into a swollen and pillared product can be characterized as involving a complex procedure, severe conditions, and unknown stoichiometry, which make the ultimate success possibly uncertain and in need of critical evaluation.¹³⁸ The possible complications can be illustrated by the already mentioned fact that, at the same time these first swelling/pillaring attempts were undertaken, in a parallel effort surfactant template M41S molecular sieves were being discovered and MCM-22/MCM-41 composites were found to exhibit many macroscopic properties similar to the pillared MCM-36. Of course, other properties allowed clear differentiation.¹³⁸ The evidence, especially details for unambiguous recognition of MCM-36 as pillared MCM-22P without M41S contaminants, can be found elsewhere.^{40,138} Briefly, MCM-36 comprises MWW layers, ca. 2.5 nm thick, separated by 2–2.5 nm interlayer space filled partially with amorphous silica (pillars) with the overall structure exhibiting mesopores in the 2.5–3.5 nm range. Successful pillaring for the entire sample was confirmed⁴³ by a combination of characterization methods: XRD, TEM, static and dynamic sorption measurements, and ultimately catalysis. The basis for distinguishing from MCM-22/M41S mixtures was also established. The initial comprehensive work identified particular features in the XRD pattern that can be applied routinely in combination with BET and related sorption results to evaluate the quality of the prepared MCM-36.⁴³

Pillared layered materials, including zeolites, are typically shown as having individual props (pillars) distributed with regularity between the layers with considerable distance/gaps between them, which is unlikely to represent the real situation. The nature of the pillars often remains unknown. The featureless appearance of interlamellar space in TEM images of cross-sectioned crystals⁴³ indicates lack of regularity and provides no further clues. The most general description can be that in between zeolite layers there is a volume of amorphous silica with channels, mainly of the size 2–3 nm, whether regular or not is unknown, but certainly allowing access to the surface of the MWW sheets. An exception to this has been claimed in the case of MFI, said to produce “pillars” that themselves have zeolite structure, that is, ZSM-5.¹⁰¹ This is quite extraordinary since silica pillared zeolites typically contain up to 50% inert component (silica) and its replacement with “zeolite pillars” is a possible further boost for activity. So far this breakthrough has not been further elaborated nor quantified.

Pillaring of layered zeolite precursors has been almost exclusively carried out using of TEOS, which seems to have a suitable rate of hydrolysis. Alternative pillaring compositions were reported by the group of Lercher.^{165–167} They used aluminum oxide alone and in combination with Ba and Mg dissolved in NaOH solutions and treated MCM-22P either preswollen or pillared with TEOS before calcination. The former was carried out at 90 °C for 4 h and the latter at 40 °C for 6 h. The final calcination was at 550 °C. There is a distinct difference in textural properties between these two groups. The swollen and pillared MCM-22P samples with new composition

show BET lower than zeolite MCM-22: 348–390 versus 432 m²/g. When the treatment was after TEOS pillaring, the BET values were between 584 and 757 m²/g compared with 711 m²/g for untreated pillared MCM-22P. The ratio of Si/Al in the composites drops below 10/1 (13/1 in MCM-22), indicative of strong “attraction of Al”. The amounts of Mg and Ba are 0.64% and 0.24%, and 2.2% and 0.24%, respectively. Characterization included NMR, IR, and temperature-programmed desorption (TPD).¹⁶⁷ The adsorption of 2,6-di-*tert*-butylpyridine (2,6-DTBPY) as probe molecule indicated an increased amount of acid sites at the pore mouth or at the outer surface of the zeolite layers compared to MCM-22. The (MgO/BaO)-Al₂O₃-SiO₂-MCM-36 showed additional Brønsted acid sites of higher strength than those in the zeolitic sheets. They were assigned to the silica–alumina clusters in the interlayer space. The presence of Mg and Ba also generated basic sites.

A novel type of pillaring was reported with arylsilsesquioxane or 1,4-bis(triethoxysilyl)benzene (BTEB).⁶⁵ It was reacted in dioxane solution with swollen MCM-22P at 80 °C for 2 days (1:1 weight ratio) under inert atmosphere and after recovery dried at room temperature (XRD showed two low-angle diffraction lines at *d*-spacing 4.45 and 3.7 nm). The swelling reagent was removed by acid extraction in two steps (one peak with *d*-spacing 4.01 nm), which appeared to have also extracted most of the original template since nitrogen content dropped from 1.5% to 0.2%. As a result of these treatments, the BET area increased from 408 to 539 m²/g, the volume of gas adsorbed increased from ~150 to 250 mL/g (at standard temperature and pressure, STP), and the mesopore volume increased from 0.07 to 0.234 mL/g, while the mean Barrett–Joyner–Halenda (BJH) pore diameter changed from microporous to 5.4 nm. The pillars comprise BTEB molecules from opposite layers coupled via (aryl)–Si-O-Si-(aryl) bridge and at the other end forming an aryl-Si-O-(MWW) connection to the layer. On the basis of organic content (10%), it was estimated that 5/8 of the surface silanol groups were occupied by bridging groups. The pillared material was further functionalized by amination. MWW-BTEB (0.5 g) was treated with a mixture of concentrated acids: 15.2 g of H₂SO₄ (98%) and 3.47 g of HNO₃ (65%) for 3 days at room temperature, and after isolation, reaction with a solution of 15 mL of HCl (37%) and 1.59 g of SnCl₂. The products were characterized by IR and NMR spectroscopies to confirm the proposed nature of obtained materials.

An alternative application of zeolite nanosheets is to develop unusual particle texture through connecting them together. The development of hierarchical porosity in zeolites has been studied for several years, with the goal of retaining selectivity of the microporous zeolite structure while improving overall mass transport and diffusion, especially of bulkier molecules, by engineering additional larger pores in the material. Many approaches to tackle this problem involve the selective partial dissolution of zeolites, the use of hard templating, or even the pillaring of layered zeolites as described above. However, MFI nanosheets can be grown in unusual “house of cards” type morphologies, which have mesoporous regions between the nanopores. Nanosheets of MFI do this through the formation of orthogonally connected nanosheets (Figure 13), described by Tsapatsis and co-workers⁶⁹ as “self-pillaring through repetitive branching”. The key to this process is the possibility of 90° twinning in the MFI structure, which leads to a change in orientation, by 90°, of the nanosheets. Figure 13 illustrates

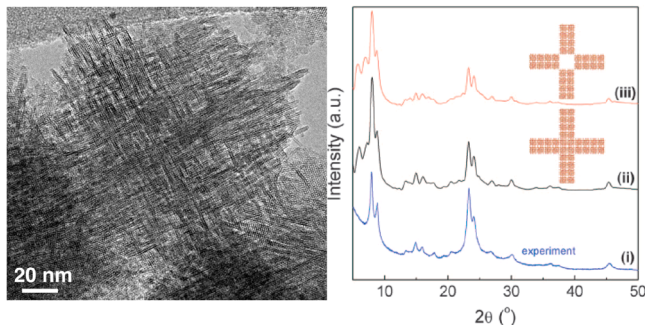


Figure 13. Self-pillared zeolites produce a “house of cards”-type structure that has a hierarchical porous structure (left panel). Two possible structural models are shown on the right, based on selective intergrowths of the zeolite structure. Reprinted with permission from ref 67. Copyright 2011 AAAS.

the house of cards arrangement of the nanosheets in a single particle and two possible structural models.

6. DELAMINATION AND EXFOLIATION

6.1. MWW Family

Delamination of zeolite layers by design, producing the material ITQ-2, with layers apparently being arranged randomly and mainly edge-to-face, was first reported by Corma et al.⁶⁶ At that time zeolite MCM-56, comprising mainly single layers in disordered packing, was already known through patent⁴⁵ and later disclosed as a delaminated zeolite by direct synthesis.⁵⁹ Other zeolites were subsequently reported as delaminated, including FER (ITQ-6),⁵³ NSI (ITQ-18),¹⁴⁷ MFI,⁶⁷ and octosilicate/RUB-18.¹⁵⁷ The conventional approach to delamination entailed preswelling under high-pH conditions as discussed above. An alternative approach under mild conditions was reported via “fluoride/chloride anion-promoted exfoliation”.^{148,168} The extent of delamination is not easy to determine, and authors usually refer to the BET area values as indicators.

The preparation of ITQ-2 is a multistep procedure:⁶⁶ swelling the MCM-22P precursor with surfactant/TPA-OH solution according to the procedure of Kresge and co-workers,^{43,44} sonication (50 W, 40 kHz) to “force the layers apart”, acidification to pH around 2, isolation of the resultant solid, and finally calcination. The product exhibits high surface area ($\sim 700 \text{ m}^2/\text{g}$), the presence of some single layers edge-on in TEM images, and other properties expected for such structures. X-ray diffraction patterns were provided and characterized as “most of the ITQ-2 layers are bent and curled (similar to clays), interfering with a detailed X-ray verification of the proposed structure”.⁶⁶ The catalytic potential of ITQ-2 was illustrated by means of a fixed-bed, small-scale catalytic-cracking test that used *n*-decane, diisopropylbenzene, and vacuum gas–oil. ITQ-2 was reported^{66,140,169} to be more active “as well as more selective than the MWW-type zeolite, yielding more of the valuable gasoline and diesel products and less gas and coke”.

Studies of ITQ-2 preparations with different Si/Al ratios showed that formation of ITQ-2 was less favorable with increasing Al content in the MCM-22 precursor.¹⁷⁰ In the series of three samples with Si/Al from 7.6 to 33.3, the highest BET area of ITQ-2 was obtained for the latter and was rather modest, $523 \text{ m}^2/\text{g}$, versus $360 \text{ m}^2/\text{g}$ in the starting material. There was also significant decrease in the Si/Al ratio to 20/1

from the initial 33/1, undoubtedly as the result of desilication due to high pH of the swelling medium. A later study confirmed that increasing Al content was less conducive to ITQ-2 formation based on samples with initial Si/Al equal to 50 or 20.¹⁴⁵ However, the quoted BET surface areas were in fact in opposite order, that is, a lower Si/Al material had greater BET values. Extensive desilication was observed and evaluated quantitatively, while the amount of sample recovered was greatly reduced due to the silica dissolution. Extending the time of sonication was also important for enhancement of the BET area of the product, but it also generated some MCM-41-type impurities in one case after 10 h.

A striking feature among the publications reporting ITQ-2, which are substantial in number, is the wide range of different and sometimes incompatible X-ray patterns attributed to this material. In practice it may mean that some materials claimed to be ITQ-2 are not the expected random collection of MWW layers. The possibilities include poorly separated layers, with significant ordering of some layers in 3D observed in crystallographic studies,^{171,172} and amorphization invoked by Katz and co-workers¹⁴⁸ as the reason for observed mesoporosity. The suggested incompatibility is judged by the fact that the X-ray pattern for a MWW material comprised a collection of disorganized/disordered single layers. It was first encountered and adopted to qualitative interpretation of the experimental pattern of the apparent MWW material designated MCM-56 (discussed later).⁴⁵ It was subsequently generated as simulated patterns^{67,173} and determined experimentally for dispersible exfoliated nanosheets from colloidal suspension. Its most salient feature appears as a prominent broad band in the range $8\text{--}10^\circ$ without a distinct trough (dip) in the middle. Such a dip is attributed to the presence of layer ordering along the stacking direction and it results in two separate peaks, (101) and (102), attributed to 3D ordered structure, such as MCM-22P and MCM-49.^{40,42} This broad band is seen in combination with reflections at 7.1° , 25° , and 26° 2θ , characteristic of MWW layer, and absence of the peak at 6.5° , typically the (002) reflection, or any significant scattering around that position. Clear examples of exactly such a pattern are seen in the aforementioned study on ITQ-2 preparation by Frontera et al.¹⁴⁵ Taking into account possible deformation and/or degradation of MWW layers upon delamination, one might see lower-quality patterns, but the lack of the distinct dip in the $8\text{--}10^\circ$ region must be viewed as required for a proper ITQ-2 specimen. These mentioned features are also characteristic for acid-treated, most likely detemplated MCM-22P material denoted MCM-56 analogue.^{61,128} The question whether in this case the evident lateral layer disorder is also associated with lack of connectivity has not been settled but it seems that the answer is negative; that is, layers may remain connected via network of hydrogen bonds.

MCM-56 denotes a MWW material⁴⁵ described as related to ITQ-2⁶⁶ and claimed to be delaminated but obtained in one-step direct hydrothermal synthesis like conventional zeolites.⁵⁹ This makes it potentially quite valuable and possibly preferred over the multistep preparations like ITQ-2, because of enormous advantage in cost and labor, of course on the condition that performance is comparable or not significantly inferior. The advantage of ITQ-2 is attributed to high surface area (e.g., $700 \text{ m}^2/\text{g}$) and “sheets being arranged randomly and mainly edge-to-face, as opposed to the face-to-face orientation attributed to MCM-56 zeolite”.¹⁴⁰ The typical BET values for

MCM-56 are in the range 400–500 m²/g. Such lower BET values compared to ITQ-2 may be viewed as a disadvantage, but on the other hand, typical MCM-56 has higher Al content, which is often reason for greater catalytic activity.¹⁷⁴ BET areas found in the literature for ITQ-2 and MCM-56 are in a quite broad range, indicating that the synthesis of high-quality materials is not yet straightforward. Results disclosed in a patent¹⁷⁵ indicate much better performance of MCM-56 compared to its nondelaminated congeners, MCM-22 and MCM-49, in liquid-phase alkylation.

The “MCM-56-like” X-ray pattern is not unique and has been obtained upon postsynthetic treatment of ordered MCM-22P with initially separate 8° and 10° 2θ peaks and a deep depression between them. These treatments were reactions with nitric acid and acetone, producing a material called “MCM-56 analogue”.^{61,140} MCM-22P is an ordered structure due to H-bonded layers with possible support from template. The formation of MCM-56 analogue can be envisioned as a collapse with loss of 3D order without breaking of the interlayer bonds. It was argued that swelling with surfactant/tetramethylammonium hydroxide may reveal the difference.²⁶ This particular mixture was reported to swell MCM-56 and presumed to be inoperative for MCM-22P. The reason for this seemed that smaller quaternary ions, like tetramethyl and ethyl, were presumed ineffective due to diffusion between the layers in MCM-22P preventing surfactant migration inside. Recent studies indicate that it is not so clear-cut and some swelling of MCM-22P with the latter mixture could be observed¹⁴³ and cannot provide unambiguous resolution.

The delamination of MCM-22P under mild conditions, pH ~9, was carried out via “fluoride/chloride anion-promoted exfoliation”.¹⁴⁸ The corresponding mixture consisted of cetyltrimethylammonium bromide, tetrabutylammonium fluoride, and chloride, with pH adjusted 9 by addition of 40% tetrapropylammonium hydroxide solution. The slurry with MCM-22P was heated at 353 K for 16 h and acidified to pH 2 with HCl, and the final isolated product was calcined at 823 K. It was designated UCB-1, while ITQ-2 was prepared alongside for comparison. XRDs of both of these materials appeared practically featureless. The authors conclude “PXRD of as-made UCB-1 ... demonstrates a powder pattern similar to that of ITQ-2 zeolite” and “the 001 (3.3, ~27 Å) and 002 (6.7, ~13 Å) peaks are significantly diminished in intensity”.¹⁴⁸ The XRD also contains extensive amorphous silica halo between 20° and 30° 2θ, suggesting low crystallographic order. Essentially only one peak that can be linked to MWW is discernible, at 26° [the (310) reflection], and is said to have a stronger intensity than for material ITQ-2. It is interpreted to suggest “a greater degree of long-range order in the direction parallel to the sheet”. The nitrogen adsorption isotherm of UCB-1 is very similar to that of MCM-22P except for the micropore and macropore region (low and high relative pressures) and exhibits analogous extended plateau at about 130 mL/g STP. In contrast, the reference ITQ-2 shows about twice the adsorbed amount in the same region. The big difference between UCB-1 and ITQ-2 is attributed to significant amount of amorphous component in the latter. The authors conclude, on the basis of TEM, that “as-made ITQ-2 zeolite shows mesoporosity that is likely a consequence of silica amorphization during delamination”. Further support for greater amorphization of ITQ-2 than UCB-1 is based on ²⁹Si NMR (Q² resonances in ITQ-2) and IR (well-resolved band at 563 cm⁻¹ assigned to pentasil rings in the framework, again with significantly diminished intensity for

ITQ-2). The particular features of UCB-1 included (i) “TEM images clearly showing curved layers, which lack long-range order”, and (ii) total uptake of nitrogen into UCB-1 and ITQ-2 at a relative pressure of approximately $10^{-7} < P/P_0 < 10^{-4}$ lower than that for MCM-22, which is consistent with loss of 10-ring during the delamination process. It remains to be confirmed by adsorption of a more suitable gas, such as argon, because nitrogen adsorption can be affected by issues such as surface roughness.¹⁷⁶

6.2. Other Delaminated Zeolites

Compared with MWW, the results concerning delamination of other zeolites are sparse and represented only by NSI, FER, and RWR (octosilicate) precursors. Zeolite NSI itself is obtained only via the indirect layered precursor route, from material NU-6(1) with 4,4'-dipyridyl as SDA separating the layers. It has been known since 1984, but its structure was recognized only in 2004.⁷⁹ The reported delamination of NU-6(1) was preceded by swelling with a quaternary alkylammonium hydroxide at pH = 12.¹⁴⁷ Cetyltrimethylammonium (CTMA⁺) treatment gave a new diffraction peak at 2.3° corresponding to a basal spacing of ca. 4.0 nm, but not all layers were expanded as suggested by the peak at 6.5°, apparently a residue of the original unexpanded precursor. It was then found that “when decyltrimethylammonium (DTMA⁺) cation was exchanged all the peaks associated with the non-expanded material disappeared and the basal spacing of the swollen zeolite was 2.85 nm indicating that the DTMA⁺ has intercalated all the layers”.¹⁴⁷ The expanded product was dispersed in an excess of water and sonicated (50 W, 40 kHz) for 1 h (“until delamination of the zeolite occurred”) and calcined at 853 K. The product was designated ITQ-18.¹⁴⁷ The structure of NU-6(2) zeolite was unknown at that time, and due to “expected poor quality of XRD spectra”, the validation of delamination was carried out through other physicochemical characterization. First, both Si NMR and IR showed the expected increase in the number of terminal silanol groups (Q³/Q⁴ increase). ITQ-18 exhibited IR bands characteristic of the zeolitic structure at 540 and 580 cm⁻¹, which was “consistent with the presence of single sheets in which short range order is retained”. The described treatment produced the expected increase in BET area: 588 m²/g with a negligible amount of micropores for ITQ-18, compared with 35 m² for NU-6(2) obtained from the same sample. Regarding the XRD of ITQ-18, despite its poorly defined profile with broad diffuse peaks, certain features are quite distinct. There is an overall similarity between XRD of NU-6(2) (calcined zeolite) and ITQ-18 despite broadening of the peaks in the latter and the absence of minor ones seen in the former. Second, even calcined ITQ-18 shows low-angle peaks with large basal *d*-spacing, which in general are not expected in delaminated materials, but it may be that the layers became self-pillared under the applied treatments. A later study on expansion of NU-6(1) showed “success and the extent of the latter (expansion) is more or less influenced by parameters like pH, hydroxide used, etc.”¹⁷⁷ On the other hand, none of the final materials after calcination showed a low-angle peak at 2θ equal to 2–3°. The other diffraction lines were in general of low intensity and according to the authors were “undoubtedly identical with the most intense diffraction lines of zeolite Nu-6(2)”. To account for the undeniably enhanced BET area (~500 m²/g) and evident presence of mesopores, it was proposed that “expanding and delaminating (including final thermal treatment) of the precursor Nu-6(1) structure causes

the formation of structure units similar to those of Nu-6(2), which are arranged in such a way that no long-range ordering is seen in the XRD patterns.¹⁷⁷

The work on delamination of the NSI precursor was extended to heteroatoms, V-ITQ-18.¹⁷⁸ The swelling was carried out with very high pH (13.8). XRD pattern of the product did not show any reflections at higher angles. The low-angle region, below $5^\circ 2\theta$, was dominated by a peak at d -spacing around 4 nm followed by smaller peaks with overall appearance resembling XRD of hexagonal mesophase MCM-41.

Delamination of the FER zeolite precursor PREFER prepared with 4-amino-2,2,6,6-tetramethylpiperidine as template was reported.⁵³ The product was designated ITQ-6. Delamination was carried out by treatment of PREFER (preswelling) with cetyltrimethylammonium bromide and tetrapropylammonium hydroxide (TPA-OH) under reflux at 368 K for 16 h. This intermediate product showed XRD dominated by a series of low-angle lines, apparently orders, characteristic of layered materials with large basal spacing. The initial (002) line of PREFER was not seen. The slurry was sonicated in an ultrasound bath (50 W, 40 kHz) at 323 K for 1 h, while the pH of 12.5 and temperature of 323 K were maintained. The final calcined solid, ITQ-6, exhibited an XRD pattern in which “the intensities of the reflections corresponding to planes (0kl) were basically unchanged compared to calcined PREFER but those corresponding to (h00) have strongly decreased”. This was considered “a remarkable loss of order along the a -axis, which would be consistent with a delamination of the layered PREFER” and “if true it indicates a delaminated structure and the resultant ITQ-6 material consists mostly of monolayers of the laminar precursor PreFER”.⁵³ The BET area increased from 270 to 618 m²/g (calcined PREFER to ITQ-6), and there was a loss of microporosity based on Ar sorption. Different levels of delamination were reported later¹⁷⁹ by changing the length of PREFER treatment, that is, for 16, 36, and 48 h, with the swelling CTMA/TPA-OH mixture at 368 K. Extending the treatment resulted in increased external surface area and diminished microporous surface area. The 48 h swelling resulted in final external surface area of 882 m²/g and no micropore contribution. These materials were tested as catalysts for *n*-hexadecane hydroisomerization. It was concluded that, with these treatments, “it is possible to prepare bifunctional acid/metal catalysts with a hydroisomerization to hydrocracking ratio and an isomers distribution that can cover a continuous range from the catalytic behavior of the purely 10 ring to the extra-large pore zeolites”.¹⁷⁹

PREFER was also delaminated by a milder approach similar to one reported for MCM-22P that used cetyltrimethylammonium bromide, tetrabutylammonium fluoride, and tetrabutylammonium chloride.¹⁶⁸ This time the solvent was *N,N*-dimethylformamide (DMF). This was the only combination (among those explored) that produced the diagnostic disappearance of the (200) reflection of PREFER at ca. $7^\circ 2\theta$. Simultaneously, additional lower and higher angle peaks appeared but were not identified with appropriate (hkl) indices. Upon acidification, which with the other reagents restored the peak around 7° , no corresponding maximum appeared but a new one showed up at ca. 6.1° . In general, only a few peaks were seen in the entire spectrum consistent with loss of order along the a -axis. The small-intensity diffraction peaks in the vicinity of 23° are attributed to $0kl$ planes consistent with preserved integrity of order within each two-dimensional

lamella. On the other hand, the significant elevated background in the range 20 – 30° is probably evidence of amorphization.

6.3. Colloidal Suspensions of Zeolite Nanosheets

Dispersion of solid lamellae in a liquid medium represents the ultimate delamination and is a desirable goal to strive for. It may not be viable for a practical large-scale implementation, at least in the near future, but its fundamental significance is undeniable. The production of colloidal suspensions of 2D solid monolayers is well-established art that has been demonstrated for many types of materials.^{180,181} In the case of layered zeolites, it is beginning to emerge as dispersible exfoliated zeolite nanosheets.⁶⁷ Zeolite precursors MFI and MWW were used in their swollen form obtained by direct synthesis and treatment of high-silica MWW (ITQ-1) with CTMA-Cl/TPA-OH mixture. The swollen precursors were exfoliated by melt blending with polystyrene (weight-average molecular mass = 45 000 g/mol) performed under nitrogen environment in a co-rotating twin screw extruder with a recirculation channel.⁶⁷ The nanosheet–polystyrene composites were mixed with toluene and sonicated. Larger particles were removed by centrifugation, yielding dispersion containing approximately 1.25% (w/w) polymer and 0.01% (w/w) nanosheets. This approach was suitable for obtaining flat, crystalline, exfoliated nanosheets. In contrast, thermal treatments to remove polystyrene resulted in substantial curling, which makes them unsuitable for use in coating and fabrication of films. The nature of the nanosheets was examined by X-ray and electron diffraction (ED) methods and microscopy [atomic force microscopy (AFM) and TEM] in combination with simulation methods. The experimental X-ray diffraction pattern of the MWW nanosheets was similar to the MCM-56^{45,59,173} and ITQ-2¹⁴⁵ patterns as well as the one simulated by the UDSKIP¹⁸² algorithm. In the case of MFI, the nanosheets were found to have about 1.5 unit cell thickness or approximately 3 nm. The suspensions have been filtered through porous supports and calcined, producing smooth zeolite films and demonstrating potential for larger-scale fabrication of membranes.

7. STRUCTURE OF LAMELLAR MATERIALS

The same experimental techniques can be applied for investigation of structural, textural, and chemical properties of 2D zeolites as those used for characterization of 3D zeolites. Some of them, however, need more detailed understanding, which is briefly shown here for X-ray powder diffraction and electron diffraction.

7.1. X-ray Powder Diffraction and Electron Diffraction

Diffraction techniques are used as primary tools for establishing the identity and atomic structure of the standard 3D zeolite frameworks. In most situations, XRD is necessary and, in conjunction with pore characterization (BET area, pore volume), a sufficient tool to confirm identity and quality of zeolite samples. It gained this status because of its relative convenience of use and completeness of the initial information it provides about crystalline solids in general. The standard application assumes idealized periodicity of the framework, that is, without defects. Zeolite framework identity is determined from positions of diffraction lines reflecting dimensions of the unit cell. Atomic structure can be obtained by detailed quantitative analysis and refinement. Additional information, like crystal size, when appropriately small, can also be obtained from peak broadening analysis.

In the area of 2D zeolites, XRD is also the initial primary tool that should be and usually is applied.^{31,40} Quantitative characterization of structures with present state-of-the-art is very limited and often impossible due to absence of the 3D periodicity and inherent disorder of the layer packing in many situations. It is reflected in diffraction patterns that are often broad, showing the 2D order of the layers but no ordering in the third dimension.¹⁴⁹ Sometimes layered zeolite precursors, that is, formally 2D zeolites, with good 3D order are available and allow complete structure analysis including atom position refinement. This is exemplified by RUB-18,⁹¹ NU-6(1),⁷⁹ or EU-19.⁷⁸ The last was in fact possible by use of single-crystal diffraction. Alternatively, the structure of the precursor is deduced from the zeolite framework it produces upon calcination. MCM-22P precursor is the most prominent example as the first such material.^{30,42} It has no properly refined structure, causing uncertainty regarding the interlayer connectivity, which has been proposed on the basis of chemical behavior^{43,124} and theoretical calculations.¹⁸³

Zeolite MWW monolayers provide a particularly rich variety of 2D structures in terms of interlayer spacing and orientation. They have been distinguished on the basis of XRD patterns, especially by the features observed in the 6–10° 2θ region.⁴⁰ They reveal interlayer spacing and lateral orientation, that is, presence or lack of vertical alignment. With the assumption that MWW layers are flat and rigid, a correlation between these features and layer packing has been proposed. The equivalent systematic analysis of other layered frameworks was proposed but so far has not been applied as broadly.

Changes in XRD patterns of zeolite crystals with diminishing size were reported in 1996¹⁸⁴ but not explicitly with regard to one dimension only, namely thickness. The approach was applied to zeolite MCM-56, considered to be delaminated MWW¹⁷³ (alternatively described as disorganized). As the framework was reduced to 1 unit cell thickness, only the intralayer ($hk0$) reflections remained well-defined and a broad band appeared in the 8–10° region instead of the distinct (101) and (102) reflections. As the crystal thickness increased, a dip began to appear in the calculated pattern at around 9°.^{59,173} The calculated pattern was similar to the experimental MCM-56 pattern, supporting its disordered monolayer character. Qualitatively analogous patterns have been seen with colloidal MWW (a new simulated pattern also generated a similar one to previous);⁶⁷ ITQ-2, produced by Frontera et al.;¹⁴⁵ and MCM-56 analogue,⁶¹ obtained by acid treatment of MCM-22P. The broad band of MCM-56 at 8–10° was also a prominent feature for swollen MCM-22P, pillared MCM-36, and disordered multilayered precursor EMM-10P.⁵⁸ The latter is also similar in overall appearance to ITQ-30,¹⁸⁵ IPC-3P,¹⁸⁶ and hexamethonium-templated MCM-22P.¹⁸⁷ On the other hand, ITQ-2 characterized by high-resolution powder X-ray diffraction data and analysis had separated diffraction lines at 8–10°,¹⁷² suggesting the sample was not fully disordered/delaminated (“lamellar stacking of only a few unit cells”).¹⁷¹ The other reported XRD patterns of delaminated MWW, as well as delaminated and pillared FER and NSI materials, are described in the section dealing with their preparation and identification.

The MWW family of zeolites, including MCM-22, MCM-49, ITQ-1, and ITQ-2 (Figure 2), was examined as a test of direct 3D structure determination by electron diffraction.¹⁷¹ It can be also seen as validation of the structural models derived by X-ray powder diffraction. Other ED determinations relevant to the

2D zeolite area include structure determination of ITQ-1¹⁸⁸ and MCM-65.⁸⁷

Other zeolite families subjected to similar analysis were IPC-3 (disordered multilayer MWW)¹⁸⁶ and PCR.⁷⁰ The calculated XRD pattern of PCR monolayer (UTL without interlayer D4R bridges) agrees well with the experimental one confirming its structural identity.

Another group of materials obtained from layered zeolite precursors that has been characterized in detail by XRD is the IEZ derivatives.⁶³ Their quantitative study has been possible because of their overall ordered nature. The bridging units form a regular pattern but in the refinement atomic positions end up displaying disorder.

7.2. Modeling of 2D Zeolites

Computational investigations of 2D zeolites have been relatively sparse; however, the number of contributions has grown in the past few years. It has been demonstrated that computational studies in combination with experiment brought new understanding of the structure and properties of 2D zeolites. Due to the size and complexity of these systems, only computationally efficient methods such as density functional theory (DFT) or force field (FF) based methods have been applied so far. Computationally simpler (and often less accurate) FF applications are briefly reviewed first, followed by applications based on the DFT method.

7.2.1. Application of Force Fields. The stacking of FER layers was modeled by use of configurational bias Monte Carlo simulations employing the CVFF force field.⁸⁸ Simulations showed that the presence of cetyltrimethylammonium cation (CTMA) leads to the rearrangement of individual layers from RUB-36 to PREFER material. Calculations have also helped to propose the mechanism behind the condensation into CDO- or FER-type 3D zeolites. The role of multiammonium surfactant in the formation of MFI zeolite nanosheets was also investigated computationally by a combination of suitable force fields.¹⁰⁴ It has been shown that $(C_3H_7)_3N^+ \cdot C_iH_{2i}^- \cdot N^+(C_3H_7)_3$ molecules, $i = 6$ and 8, both have stabilizing effect on the bulk lattice and both are preferably located along the straight channel.

The accuracy of these results strongly depends on the quality of the force fields employed. The reliability of force fields for the description of 2D zeolites has not been fully established yet. The performance of two potentially suitable force fields specifically parametrized for the description of the hydroxylated silica surfaces was tested recently:¹³⁰ (i) FFSiOH, a polarizable core–shell model force field by Pedone et al.,¹⁸⁹ and (ii) modified ClayFF¹⁹⁰ force field (modClayFF), a nonpolarizable force field based on ClayFF and modified by Bushuev and Sastre.^{191,192} The interaction of IPC-1P layers were found to be strongly overestimated with FFSiOH with respect to the reference vdW-DF2 calculations (see below), while modClayFF gave interaction energies in good agreement with vdW-DF2 ones.¹³⁰ However, relative energies of various interlayer arrangement obtained with modClayFF did not agree with those obtained at the vdW-DF2 level (for details see Supporting Information of ref 130).

7.2.2. Application of Density Functional Theory Methods. The transition from layered zeolite precursor MCM-22P into 3D zeolite MCM-22 was modeled by means of simple cluster model calculations (using BLYP exchange–correlation functional, small basis set, and small cluster model consisting of a few tens of atoms).¹⁸³ The interlayer hydrogen

bonding was found to be critical for the layered material model, and an interlayer distance decrease of 0.27 nm was calculated upon the formation of fully connected 3D MCM-22 framework. Such a large change of interlayer distance is in sharp contrast to the reported experimental average value of 0.16 nm.⁴² It has been suggested by the authors that this discrepancy may be due to the fact that experimental MCM-22P material is already partially connected by covalent Si—O—Si bridges. However, due to the rather approximate character of models and methods used in ref 183, it cannot be excluded that the discrepancy is due to the model and methods used (small size of the cluster model and complete neglect of dispersion interactions in particular). Partial connection is also less probable in view of the experimental facts: (i) the layers can be separated by swelling and (ii) an expanded IEZ structure is not possible if there are already extensive T—O—T links between the layers.

Structures of zeolite nanosheets having MWW and MFI topology were computationally investigated at the DFT level by use of periodic models and PBE exchange–correlation functionals.⁶⁷ It was shown that the structures of these nanosheets are very similar to those of the corresponding 3D zeolite; in particular, the thickness of the MFI sheet is almost identical with the thickness taken from 3D zeolite (3.20 and 3.21 nm, respectively), and also rather similar values of 2.63 and 2.49 nm were found for 2D and 3D MWW material. Note, however, that only atoms close to the slab (layer) surface were allowed to relax and that the model of isolated single 2D slab in vacuum was adopted. XRD patterns were simulated by use of 50 × 50 nanosheets with varying thickness. Simulations show the best agreement with experimental XRD patterns for MWW and MFI slabs with thickness 1 and 1.5 unit cells, respectively, in agreement with experimental results (high-resolution TEM).

New understanding of the properties of 2D zeolites has been reported recently in a series of papers by Sauer and Freund and co-workers.^{108,193–195} The differences between 2D and 3D zeolites were reported on the basis of a combination of various experimental techniques and computational investigation employing periodic DFT models. The preparation of 2D aluminosilicate thin films that do not contain external silanol groups on the metal substrates (briefly described below) opened up the possibility to investigate zeolites via surface science techniques (e.g., scanning tunneling microscopy, low-energy electron diffraction, or helium ion scattering spectroscopy). Thus, the catalytic centers, “hidden” inside the pores in 3D zeolites, become visible for surface science techniques.

The structure of bilayer aluminosilicate film formed on Ru(0001) surface was investigated by X-ray photoelectron spectroscopy, scanning tunneling microscopy, and infrared reflection spectroscopy together with extensive DFT calculations.¹⁰⁸ Similarly as in the case of silicate bilayers, the aluminosilicate bilayer on Ru(0001) appears to be a 2D array of double-six-member rings (D6R) with no Si(Al)—O—Ru bridges formed between aluminosilicate and the support. Aluminum atoms preferentially occupy positions in the lower aluminosilicate layer [adjacent to Ru(0001) surface] where the charge balance is provided by the metal substrate. Aluminum in the lower layer does not exhibit any Brønsted acidity. Only for the Si/Al ratios smaller than 4 were aluminum atoms in the upper layer observed. The presence of Al in the upper layer leads to the formation of bridging hydroxyl groups; the hydroxyl group formed on the oxygen atom in the upper layer was found to be energetically the most stable and it shows calculated OH

stretching frequencies in agreement with experimentally observed frequencies of 3594 cm⁻¹. This 2D array of D6R-containing bridging hydroxyl groups was denoted as H-2dH.

The interaction between the silica bilayer and the Ru(0001) surface was investigated at the DFT-D level; an adhesion energy of about 3 kJ·mol⁻¹·Å⁻² has been reported.¹⁰⁷ The acidity and the adsorption of probe molecules on Brønsted sites of the 2D aluminosilicate bilayer were investigated at the DFT level of theory and by infrared reflection absorption spectroscopy.¹⁹⁴ The results obtained for H-2dH layered zeolite were compared with those obtained for H-CHA, a zeolite that can be viewed as a 3D array of D6R units. The interactions with weak bases (CO and C₂H₄) and strong bases (NH₃ and pyridine) were considered. Geometry optimization and interaction energy calculations were performed with periodic model and PBE functional augmented with a semiempirical 1/r⁶ dispersion term (PBE+D). Vibrational frequencies of hydroxyl groups and of adsorbed CO molecules were calculated by the ω/r correlation method.¹⁹⁶ In agreement with experimental observation, calculations showed that (i) interaction of strong bases with H-2dH layer results in proton transfer from Brønsted site to the base; (ii) interaction of weak bases with Brønsted acid sites in the H-2dH layer leads to a larger red shift in OH stretching frequencies than found for H-CHA, indicating a higher acidity; and (iii) larger adsorption enthalpies were calculated for weak bases adsorbed on H-CHA than on H-2dH.

The interaction between layers of recently discovered layered zeolite framework IPC-1P⁷¹ was investigated computationally by employing both cluster and periodic models and various levels of theory including the coupled cluster method (cluster models) and DFT and force fields (periodic models).¹³⁰ The suitability of computational methods for the description of interlayer interaction in layered zeolites was investigated first, with coupled cluster results obtained for interacting cluster models (containing one to three Si atoms) as the benchmark. The results obtained with vdW-DF2 functional¹⁹⁷ were found to be in good agreement with reference coupled cluster results, while those obtained with other investigated nonlocal exchange–correlation functionals (optPBE and optB86b¹⁹⁸) and with semiempirical dispersion correction (PBE-D2¹⁹⁹) overestimate the interlayer interaction by about 10–20%. On the contrary, the semilocal functional without dispersion corrections underestimated the interlayer interaction (performance of force fields was discussed above). The interlayer interaction was investigated with the periodic model and nonlocal exchange–correlation vdW-DF2 functional. The energetically most stable arrangement of IPC-1P layers is depicted in Figure 14. The interaction is controlled by interlayer hydrogen bonds (H-bonds) formed between silanol groups on adjacent layers. Relatively large density of surface silanols in IPC-1P (about 1 silanol/43 Å²) results in the existence of a large number of interlayer arrangements (Figure 15). Structures with the largest number of interlayer H-bonds are the most stable (one H-bond accounts on average for about 25 kJ·mol⁻¹); up to three H-bonds can be formed between two pairs of silanol groups located on adjacent layers (Figure 15). Note that the most stable arrangement of IPC-1P layers obtained at the vdW-DF2 level of theory (depicted in Figure 14) corresponds well with experimental data: (i) distance between two adjacent layers obtained experimentally and computationally is 10.7 and 10.8 Å, respectively, and (ii) this arrangement corresponds to the PCR zeolite obtained experimentally upon the condensation of IPC-1P material by

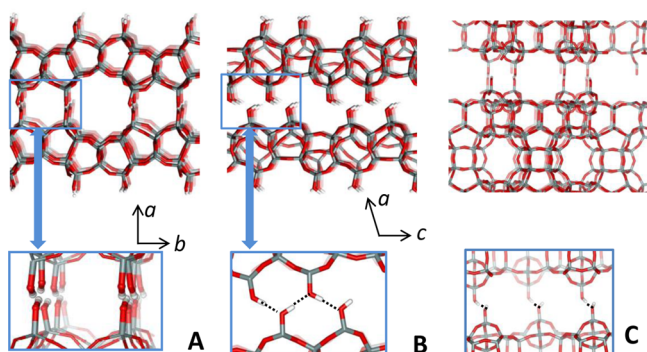


Figure 14. Interaction between 2D zeolite layers is dominated by interlayer hydrogen bonds. (A, B) Large density of surface silanol results in the formation of hydrogen-bonded networks. (C) Significantly lower concentration of surface silanols in MCP-22P only allows the formation of isolated interlayer hydrogen bonds. Silicon, oxygen, and hydrogen atoms are depicted in gray, red, and white, respectively.

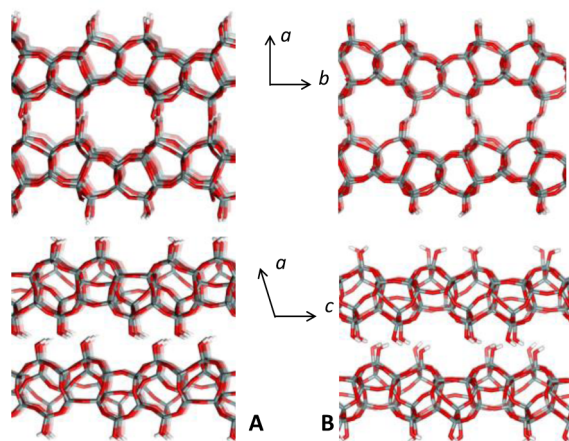


Figure 15. Two examples of interlayer arrangement of IPC-1P layers. A maximum number of interlayer H-bonds is formed in both cases. Structure B is shifted along the *b* axis by about half the corresponding UC vector with respect to structure A. Upon condensation, structure A leads to a zeolite with 10R along *c* (zeolite PCR in this particular case), while structure B would lead to a different zeolite containing an 8R along *b*. Silicon, oxygen, and hydrogen atoms are depicted in gray, red, and white, respectively.

calcination.⁷⁰ The interlayer interaction is characterized by adhesion energy of $1.0 \text{ kJ}\cdot\text{mol}^{-1}\cdot\text{\AA}^{-2}$; about 80% of interaction energy is due to hydrogen bonding, and the remaining 20% comes from the dispersion. The effect of octylamine (OCA) structure directing agent on the ordering of IPC-1P layers was also investigated computationally.²³ OCA was placed between two IPC-1P layers; geometry optimization (relaxing positions of all ions) was performed for several initial placements of OCA between two IPC-1P layers. Calculations showed that the energy differences between various interlayer arrangements increased. The effect of water on the interlayer interaction is certainly also very important; however, it has not been considered so far for the interacting zeolite layers. Some information can be obtained from extensive literature on the water interaction with various silica surfaces.^{200,201}

While the nonlocal vdW-DF2 functional was shown to provide accurate results for the interlayer interactions in 2D zeolites,¹³⁰ its use for the description of adsorption of

molecules on the 2D zeolites is somewhat less reliable.²⁰² The most accurate computational method used so far to investigate properties of 2D zeolites was used in the theoretical investigation of adsorption of small molecules (CH_4 , CO_2 , H_2O , H_2 , and N_2) on layered zeolites;²⁰² in particular, these systems were investigated by a modified DFT/CC method.^{203,204} Careful evaluation of the accuracy of DFT-D2¹⁹⁹ and vdW-DF2¹⁹⁷ with respect to reference coupled cluster calculations showed that both approaches tended to overestimate the interaction with the surface, while DFT/CC results were in excellent agreement with reference data. This overestimation leads (in some cases) to qualitatively wrong prediction of preferred adsorption sites. The adsorption on 2D zeolites derived from UTI and ITH, denoted 2D-UTI and 2D-ITH, respectively, was considered. While 2D-UTI is already an experimentally known material (IPC-1P⁷¹), 2D-ITH has not been prepared experimentally yet. The 2D-ITH layers contain 9R channels through the lamella, contrary to 2D-UTI layers. The binding energies on the 2D-ITH sites were larger than those on the corresponding 2D-UTI sites for the following reasons: (i) silanol islands are closely packed in 2D-ITH (there is one silanol group per 32 and 44 \AA^2 on 2D-ITH and 2D-UTI, respectively); (ii) the surface of 2D-ITH is more flat than that of 2D-UTI and that corresponds to larger dispersion interactions; and (iii) a larger framework density in some parts of 2D-ITH (2D-UTI and 2D-ITH have similar framework densities, but the distribution is less homogeneous in 2D-ITH containing 9R windows). Except for methane, all other molecules preferably bind on the group of four surface silanols that are the remnants of D4R units of the parent 3D zeolite; methane preferably binds in between two silanol quartets. Interaction energies on the 3D ITH zeolite and on the 2D-ITH layer were also investigated. Interaction of methane with 3D zeolite is stronger than the interaction with corresponding sites on 2D-ITH due to increased material density and thus increased dispersion interactions. Note, however, that the calculations on 2D zeolites were modeled by individual layers separated by vacuum. On the contrary, for molecules possessing permanent dipole or quadrupole moments, the interaction with 2D-ITH is stronger than with ITH due to the presence of surface silanol groups, resulting in stronger electrostatic interactions. The inaccuracy in DFT-D and vdW-DF2 description of these system was demonstrated on energy profiles for methane passage through the 9R window of 2D-ITH; both methods gave the path in qualitative agreement with DFT/CC, but the barriers are almost 100% overestimated.

8. TWO-DIMENSIONAL ZEOLITES IN CATALYSIS

A major objective in exploration of zeolite nanosheets is the development of novel catalysts. To probe the effect of reduction of crystallite thickness on catalytic properties, several different classes of catalyst have been tested: solid acid catalysts, titanosilicate oxidation catalysts, and supports for metal nanoparticles, to name but a few. Phosphorus-31 NMR studies on adsorbed species on the nanosheets showed that the external acid sites are different from those present on the internal surface and that there is a linear correlation between the number of the strongest external acid sites and activity for the cracking of large hydrocarbons.^{205–207} This can be seen also for toluene disproportionation and alkylation with 2-propanol.²⁰⁸ Changing the number and type of acid sites available, using nanosheets rather than bulk crystals, significantly changes the diffusion properties of substrates within the solids.²⁰⁹ For

example, in *n*-heptane hydroisomerization, catalyzed by zeolite-supported Pt nanoparticles, the nanosheets had significantly higher selectivity toward the branched hydrocarbons compared to bulk crystals, which was attributed to the easy diffusion of the branched molecules, reducing the chances of competing cracking reactions.

Morphological effects of two-dimensional zeolites were investigated in different organic reactions. The ultimate goal of these studies is to provide improved performance through higher activity or selectivity, or both, of 2D zeolites with respect to conventional zeolites. In principle, 2D zeolites can be efficiently used as catalysts for reactions of bulky substrates that cannot enter zeolitic pores but require active sites of zeolitic type. Significant enhancement of the reaction rate can be achieved with 2D zeolites having active sites on the surface due to a substantial increase in mass transfer. In contrast, 2D zeolites do not generally possess micropores, or if they do they are rather short. As a result, shape-selective effects can hardly be expected in a similar way to zeolites.^{210,211}

Generally, the catalytic performance of novel 2D catalysts is compared with that of “conventional” 3D zeolite samples, which may in some cases be a rather difficult comparison. Detailed studies of the effects of crystal size, concentration, and accessibility of active sites in “conventional” zeolites with respect to 2D zeolites are necessary for better understanding of the advantages and disadvantages of individual materials. Although the number of papers dealing with investigations of acid strength on external versus internal surfaces is rather limited, Ryoo and co-workers²⁰⁵ identified three types of Brønsted acid sites with different acid strengths on the external surface by use of ³¹P NMR. A linear correlation between the number of strong acid sites and catalytic activity in decalin cracking was established for layered MFI zeolite.

Catalysts under study can be divided into two groups on the basis of their textural and chemical properties. While delaminated zeolites are in principle composed of only one type of material (i.e., zeolite monolayers), pillared zeolitic materials consist of not only zeolite layers but also inorganic (organic) pillars. As a result, the “whole” external surface of delaminated zeolites can serve as a catalytically active region while inorganic pillars (silica, magnesia, etc.) are inactive and simply dilute the concentration of active sites. The targeted functionalization of amorphous inorganic pillars has been quite limited. In contrast, organic pillars can be without functionalities or functionalized to provide acidic or basic sites.^{65,212} On the other hand, inorganic-only pillared materials can be thermally activated as standard zeolites, which is not acceptable for organic pillars or SDA-filled intralayer pores.

The first evidence of enhanced catalytic performance came from pillared MCM-36.^{68,213,214} It should be noted that standard MCM-36 contains roughly 50% by weight of amorphous silica, which is inactive in many processes, and MCM-36 is effectively “diluted” MCM-22 zeolite. However, the pillaring demonstrated its benefits nonetheless as MCM-36 was reported as effective, and better than MCM-22, in olefin alkylation of isobutane, which is an important industrial process currently used in refineries with HF and sulfuric acid as catalysts. The high performance of MCM-36 was manifested, in contrast to other zeolites, in its resistance to deactivation.

Corma et al.⁶⁶ showed that delaminated ITQ-2, which is another form of zeolite MWW, exhibited similar conversion as MWW but a higher selectivity to liquid products in decene cracking. Higher accessibility of acid sites and shorter diffusion

paths in ITQ-2 were appreciated for bulkier molecules as feedstocks. The ITQ-2 sample is more active as well as more selective in transformation of vacuum gas–oil over MWW zeolite, yielding more of the valuable gasoline and diesel products and less gas and coke.⁶⁶ Utilization of MWW layers for the preparation of pillared MCM-36 was discussed by Maheshwari et al.,²¹⁵ who reported a gentle swelling and pillaring process to prevent destruction of the MWW zeolitic layers. As a result, higher conversions of MCM-36 were achieved in vacuum gas–oil cracking²¹⁵ in comparison to the original MCM-22. The reported mild swelling conditions are not as effective with high-Al MCM-22 precursor, which in principle affords more active catalysts. Thus, there is the need to compare the less degraded low-Al MCM-36 specimen with the more Al-rich one but obtained via more severe potentially damaging swelling regime.

ITQ-2 prepared from MWW lamellar precursor and having surface areas larger than 700 m²·g⁻¹ showed superiority over MWW and MCM-36 in vacuum gas–oil cracking. ITQ-2 exhibited higher conversion and yield of gasoline than other catalysts and similar yield of diesel as MCM-36. ITQ-2 is also highly active in reactions leading to the preparation of fine chemicals.

8.1. Petrochemistry

Transformations of aromatic hydrocarbons form the “heart” of petrochemistry. In theory, the open structures of 2D zeolites offer advantages through easy diffusion of reactants and products. It was apparently revealed in a liquid-phase benzene alkylation with ethylene to ethylbenzene over MCM-56, which is a delaminated zeolite from direct synthesis, tested under industrial conditions and disclosed in a patent.²¹⁶ As shown in Figure 16, 2D zeolite MCM-56 exhibited greater activity when

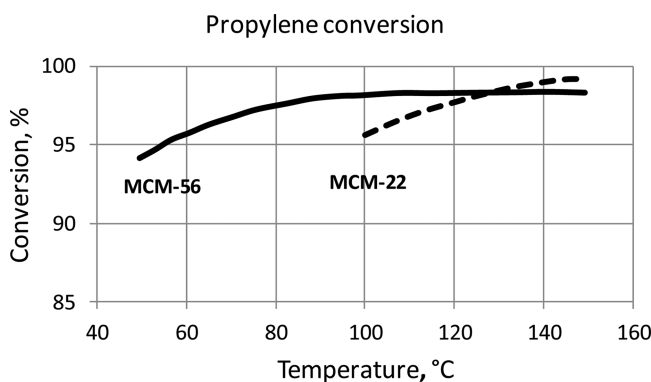


Figure 16. Benzene alkylation with propylene in liquid phase. MCM-56 shows the same conversion at the reaction temperature lower by 45 °C in comparison with MCM-22.¹⁷⁵ Benzene/propylene = 3 (mol/mol), 300 psig, propylene weight hourly space velocity (WHSV) equal to 2.5 and 1.3 h⁻¹ for MCM-56 and MCM-22, respectively. Zeolites were alumina-bound with ratio 65/35 (w/w).

compared with conventional 3D zeolites possessing the same layer structure, namely, MCM-22 and MCM-49. Under different conditions, MCM-56 demonstrated another side of layered/delaminated zeolites: sensitivity to deactivation/degradation as reported by Juttu and Lobo.¹⁷³ The sample activated by apparently standard treatment accorded to other zeolites proved to be deformed and showed inferior activity compared to the conventional MCM-22. Clearly, much remains to be

learned about handling and activation of 2D zeolites in order to optimize their effectiveness.

Cumene²¹⁷ and cymene²¹⁸ syntheses were investigated over MWW zeolites with different Si/Al ratios. Kinetic runs suggested that the reactions proceed mainly at the external surface, most probably in the cups of MWW zeolite. These results evidenced the importance of the structure of the external surface of zeolites, particularly in connection with lamellar zeolites. In the case of cumene synthesis by benzene alkylation with propylene²⁰⁶ over nanomorphic zeolites BEA, MTW, and MRE, having large external surface areas, higher activity and long catalytic lifetime were achieved in comparison with conventional zeolites of the same zeolite type. Short zeolite channels and a high concentration of acid sites on the external surface contributed significantly to the zeolite activity. No *n*-propylbenzene was found among the reaction products due to the large-pore zeolite systems investigated and contribution of the external surface, which confirm the proposed reaction mechanism over medium-pore zeolites with intersecting channels, like MFI or MEL.^{219,220} A different situation was observed when the activity of lamellar MFI zeolite in toluene disproportionation and its alkylation with isopropyl alcohol was compared with related mesostructured zeolites probably having also 10-ring channels.²⁰⁸ Although substantially increased concentration of acid sites on the external surface was evidenced by adsorption of 2,6-di-*tert*-butylpyridine, the contribution of the zeolite channel system was significant. Lamellar MFI zeolite formed only by two layers exhibited high para selectivity as well as low *iso*-/*n*-propyl ratio in cymene products, providing evidence of significant contribution of reactions proceeding inside the zeolite channel system. Transformation of cymenes to *n*-propyltoluenes proceeds in the intersections of 10-ring channels,^{221,222} and the size of intersection controls the selectivity of the reaction.²²³ In addition, two-layers of MFI zeolite enhance the para selectivity in the formation of *p*-cymene in contrast to *p*-xylene in toluene disproportionation.²⁰⁸

MWW zeolite offers an interesting comparison with its structural analogues having the same layer structure, namely, pillared MCM-36, delaminated ITQ-2, and MCM-56.¹⁴⁰ To investigate the effect of textural features of MWW zeolite, *m*-xylene transformation was used.²²⁴ Pillaring of MCM-22P substantially changed the course of the reaction: about 15% of *m*-xylene transformation occurred in the 10-ring intralayer pores in MCM-36 compared with more than 70% in the parent MWW sample. The main part of the reaction (85%) over MCM-36 proceeds in surface pockets accessible to larger molecules.²²⁴

Delaminated zeolite ITQ-2 was studied in methane dehydroaromatization to aromatics and compared with MWW, both supports modified with Mo.²²⁵ The purpose of this study was to decrease the rate of deactivation when lamellar ITQ-2 was used in comparison with conventional MWW zeolite. ITQ-2 produced more naphthalene and less benzene than MWW, and the selectivity to benzene was substantially improved by surface dealumination of ITQ-2.²²⁵ Experimental results of dealumination and molecular dynamics simulation provided some evidence that naphthalene is primarily formed on the active sites on the external surface of ITQ-2.

Modification of ITQ-2 with Ni, Mo, or Pt resulted in the preparation of catalysts highly active in mild hydrocracking and aromatic hydrogenation.²²⁶ The catalysts benefit from the

peculiar structure of ITQ-2 zeolite combining high activity of zeolites with desired selectivity of amorphous catalysts. Minimization of diffusional problems in 2D ITQ-2 is expected to favor this catalyst over microporous MWW. Delaminated zeolites ITQ-2 (MWW-type), ITQ-6 (FER-type), and ITQ-18 were found to be efficient for the synthesis of diaminodiphenylmethane (DADPM), an important precursor in the manufacture of polyurethanes.²²⁷ The exfoliation substantially increased the accessibility of active sites, making adsorption and desorption of reactants and products much easier.²²⁸ It seems that the topology of the delaminated zeolite controls the isomer distribution, offering additional flexibility in the synthesis of DADPM.

One can benefit from the lamellar structure of ITQ-2-based catalysts over conventional ones also in the case of Fischer-Tropsch synthesis. As reported by the group of Martínez and co-workers,^{229,230} cobalt-supported ITQ-2 and ITQ-2 lamellar zeolites were superior over SBA-15 related mesoporous catalysts having comparable BET areas.²³¹ Similarly, Co-ITQ-18 was reported as an efficient catalyst for bioethanol steam reforming. Structure of ITQ-18 layers stabilized the dispersion of Co particles and prevented their sintering.²³² ITQ-6 structure stabilizes Ni particles in methane dry re-forming at a reaction temperature of 700 °C. Methane conversion of 80% and CO₂ conversion of about 90% were achieved, providing synthesis with H₂/CO ratio 1.4 after 30 h of time-on-stream.²³³

Surfactant-directed zeolite nanosheets with the MFI structure exhibit remarkably long catalytic lifetimes and high selectivity in gas-phase Beckmann rearrangements.²³⁴ A large external surface with a high concentration of silanol groups makes this two-dimensional zeolite remarkable in the production of ϵ -caprolactam from cyclohexanone oxime.

8.2. Oxidation Reactions

Two-dimensional MFI zeolites were also modified by isomorphous substitution with iron or titanium, in addition to aluminum incorporation, to provide some redox properties. Iron-modified sheetlike MFI zeolite exhibits high catalytic performance in benzene oxidation with nitrous oxide to phenol.²³⁵ Sheetlike (Fe)MFI zeolite displays high activity in benzene oxidation due to the presence of monomeric Fe species, and the rate of deactivation decreases with decreasing Fe content.

Introduction of Ti into lamellar zeolites is beneficial in the case of epoxidation reactions of bulky substrates. Ti-ITQ-2 showed high activity and selectivity in epoxidation of olefins with organic hydroperoxides.²³⁶ Similarly, incorporation of Ti into the lamellar structure of ITQ-6 (FER structure) provided a highly active epoxidation catalyst.²³⁷

Corma et al.²³⁷ demonstrated that Ti-ITQ-6 is more active than Ti-FER or Ti-BEA in hexene and norbornene epoxidation. Delaminated titanosilicates also provide high catalytic performance when hydrogen peroxide is used as oxidation agent.^{238,239} The tetrahedral coordination of Ti in the zeolite was responsible for high stability of the conversion. Delaminated Ti zeolites were also active in cyclooctene and cyclododecene epoxidations as evidenced by Wu and Tatsumi.²⁴⁰ Structural features of MWW analogues with tetrahedrally coordinated titanium are responsible for exceptional activity in oxidation reactions.^{62,160,241,242} Titanium-containing lamellar MFI zeolite synthesized with surfactant C₁₆H₃₃-N⁺(CH₃)₂-C₆H₁₂-N⁺(CH₃)₂-C₆H₁₃ is also highly active in epoxidation reactions, in particular with bulky substrates when hydrogen peroxide or

tert-butyl hydroperoxide is used as oxidant.²⁴³ The authors concluded that Ti sites on the external surface contribute significantly to the catalytic activity, while further treatment with ammonium fluoride reduces the concentration of surface silanol groups and thus increases surface hydrophobicity.

8.3. Fine Chemical Synthesis

BEA and MWW exhibited similar performance as ITQ-2 in dimethylacetal formation and tetrahydropyranylation of alcohols and phenols.^{182,244,245} In contrast, the performance of ITQ-2 was superior to that of other zeolites for bulkier substrates not accessing zeolite channels. In acetalization of 2-acetyl naphthalene with propylene glycol, the yield increased in the order BEA (5%) < MWW (20%) < ITQ-2 (63%).¹⁸² In contrast, to lamellar materials derived from MWW, FER, or MFI, other zeolites were much less studied as for their catalytic properties. As an exception, Lima et al.²⁴⁶ tested delaminated zeolite derived from the layered material Nu-6(1) in the liquid-phase cyclodehydration of xylose to furfural. This delaminated catalyst exhibited xylose conversion of about 80–85%.

8.4. Organometallics

Large external surfaces of two-dimensional zeolites offer the possibility of their modifications with organic or organometallic moieties in similar way as mesoporous molecular sieves;^{247,248} however, only a few studies were reported in the literature. Delaminated materials can be used for adsorption or catalysis with remarkable results. Functionalization of ITQ-6 with organic amines provided excellent adsorbent for CO₂ capture, more efficient than similar modified SBA-15 materials when relating to CO₂/amine ratio.²⁴⁹ This result was explained in terms of more appropriate organization of individual amino-propyl groups on the “flat” surface of delaminated material in comparison with the less structured surface of SBA-15. External surface of delaminated materials ITQ-2 and ITQ-6 was modified by organometallic Schiff base complexes for Heck and Suzuki coupling reactions.²⁵⁰ Addition of palladium acetate provided catalysts with high activity and recyclability without leaching. Continuing this research, Corma et al.²⁵¹ immobilized mononuclear asymmetrical N-heterocyclic carbene–gold complexes on delaminated ITQ-2. These complexes exhibit TOFs up to 400 h⁻¹ in hydrogenations of alkenes and Suzuki coupling without dramatic deactivation. In another work, high activity in ethylene polymerization was reached over zirconocenes Cp₂ZrCl₂ and (nBuCp)₂ZrCl₂ grafted to ITQ-2 and SBA-15, with methylalumoxane used as cocatalyst. Mesoporous catalyst exhibited higher activity, probably due to a larger external surface.²⁵²

Delaminated ITQ-2 was modified with Ru(bpy)₃²⁺ on the external surface to demonstrate through-framework electron transfer in this system.²⁵³ External surface of delaminated zeolites ITQ-2 and ITQ-6 can be used for immobilization of enzymes β -galactosidase from *Aspergillus oryzae* and penicillin G-acylase (PGA) from *Escherichia coli*.^{226,254} The immobilized enzymes are highly stable when bound by electrostatic and covalent interactions while preserving enzymatic activity.

Three chiral Mn(III) salen complexes were anchored to MCM-41 and delaminated zeolites ITQ-2 and ITQ-6. It was shown that the orientation of the complex with regard to the surface plays a critical role in the activity, while the adjustment of hydrophobicity controls the selectivity to epoxidation.²⁵⁵ Delaminated ITQ-2 can also serve as a support for modification with different amines accommodating Pd for C–C coupling reactions.²⁵⁶ In particular, this catalyst serves as a source of

catalytically active metal species for the Heck reaction of *n*-butyl acrylate with bromobenzene proceeding in the liquid phase.

9. CHALLENGES AND OPPORTUNITIES

The phenomenon of layered (2D) zeolites emerged about two decades ago as a novel expression of the frameworks that until then had been regarded only as 3D solids. It represents a profound fundamental expansion, signifying potentially general phenomena encompassing most, maybe even all, existing zeolite frameworks. From that perspective, the traditional 3D zeolites would be a subgroup of the broader area of materials constructed from zeolite layers as the primary building blocks and enabling diverse porous structures, especially including micro- and mesoporous hybrids.

On the practical side, lamellar zeolites bridge the gap between conventionally separate classes of 3D frameworks and 2D solids. They combine useful benefits of both classes: high catalytic activity, microporosity (although not in all 2D materials), thermal stability, and chemical resistance of zeolites with structural flexibility of 2D solids, enabling their postsynthetic modification, both structural and compositional. To date, about 5% of 213 recognized zeolite frameworks demonstrated 2D character, affording materials with layers of approximately 1 unit cell thickness. Fifteen unique layered zeolite forms, including 3D frameworks, have been recognized so far, some represented by only a single example. In some cases, like self-pillared (MFI), the formation is rationalized by the particular features of the framework allowing continuous intergrowth with zeolite MEL. Despite that, we do not rule out the possibility that this special form and others that seem unique may be possible for other frameworks.

The main category of 2D zeolites is the layered precursors, which are viewed as primary forms because they are the starting materials for further modifications. The various modifications may be an end product (IEZ-stabilized) or they may be further modifiable, like intercalated and swollen derivatives. The latter may be transformed into pillared, delaminated, or colloidal suspensions. The precursors are predominantly multilayered, but there is an example of monolayered MCM-56 obtained by one-step synthesis like regular zeolites. It would be desirable to synthesize other frameworks as modifiable delaminated structures by an analogous approach. Synthesis method, either via direct synthesis or by postsynthetic modification, is another criterion for classifying layered zeolite materials. The latter offers a variety of highly desirable species like expanded or more open structures. Postsynthetic modification may ultimately prove impractical in many cases or less competitive with directly synthesized materials because of tedious multistep preparation procedures and associated high cost.

New precursors can also be obtained from a regular zeolite by selective chemical degradation. It is based and proven on exploiting possible weaknesses in frameworks like D4R units enriched with Ge heteroatoms. Very rich and novel modifications and phenomena were revealed by this approach. The synthesis of MFI as single-unit-cell nanosheets is particularly notable and promising as the source of new layered precursors. It entailed the use of a structure-directing agent prepared specifically for that purpose, which indicates the potential of synthesis by design. Additionally, structure of the template can control the thickness of MFI layers.

The main synthetic effort has been focused on the extension of various layered forms to other frameworks. It is also

significant that well-established zeolites known as minerals, like FER and SOD and especially the above-mentioned MFI, demonstrated synthetic layered forms. Synthesis of the layered precursors is especially important because subsequent modification procedures are fairly well developed. Characterization goals and methods are quite similar to those for standard zeolites but the level of complexity is much higher, especially with regard to structure, as many are disordered. X-ray powder diffraction is very useful as the primary identification tool but often must be supplemented with other techniques, including microscopy and porosity determination. Even then, some structural features, especially in very disordered layered materials, are difficult to discern and prove.

In the area of catalysis, the layered zeolites have the potential to afford expanded or more open porous structures with increased access of reactants that are too big for micropores of standard zeolites. There are many reports about enhanced performance achieved with modified materials, especially delaminated and pillared materials. This is very encouraging, but the potential for wider, especially larger-scale use must take into account more complex and costly preparation procedures that the postsynthetic delamination and pillaring entail. An additional impediment comes from the fact that implementation of new synthetic approaches involves overcoming the usual barriers of doing something for the first time. The small size (thickness) of the layers is likely to make them more unstable thermally and chemically. This justifies a bigger focus on fundamental comparison of the layered zeolite derivatives with the standard zeolites in terms of chemical kinetics, stability, etc. It is reinforced by the fact that, in many cases, state of the art of industrial catalyst is not available for comparison. As example, we can point to MCM-56, which appeared very promising from the results presented in patents. In the laboratory, MCM-56 was found to be susceptible to degradation and deactivation, resulting in disappointing performance.

The new issue as well as opportunity in exploitation of 2D zeolites is associated with formulation into a functional catalyst, for example, bound with additives that would be required in a larger-scale application. This appeared as a minor problem when working with conventional compact 3D zeolite crystals and has not been studied much, except maybe in the industry where it has a direct impact. Such results usually do not enter the public domain. In addition, the processes of catalyst formulation require specialized equipment that is not readily available and is difficult to operate in academic laboratories. The problems of larger-scale use and scale-up are now approached systematically in connection with hierarchical zeolites.²⁵⁷ New insights are developed thanks to application of detailed characterization and visualization methods.²⁵⁸ These findings can be extended to solving problems such as avoiding collapse of expanded structures. Virtually nothing is known about it directly, although some useful hints can be already identified, mainly through rare publications on related problems from the industry. Thus, the excellent performance of alumina-bound MCM-36 in isobutene alkylation can be understood as indicating that its pillared structure did not collapse in the pressure and heat of extrusion.²¹³ Similarly, the successful scale-up of MCM-41 indicated that nontrivial problems of burning off large amount of surfactant from large pore structures can be resolved.²⁵⁹ The mentioned treatments and operations are not only sources of problems but may also lead to an advantage, as reported for MWW crystal that were extruded, jet-milled, and subject to other potentially degrading treatments. It was

observed that, in contrast to standard samples showing mainly flat-on crystal orientation, the treated ones contained many edge-on crystals.²⁶⁰ This apparently more random spatial orientation and maybe some fragmentation may contribute to high performance, for example, as for MCM-56 mentioned in the preceding paragraph.

In the area of characterization, the challenge is to better understand and be able to analyze quantitatively the X-ray diffraction and related techniques of structural analysis. There is no uniform approach to analyze and present results. The MWW zeolite family has been extensively studied by XRD and showed great potential in identification of various structures. The extension of this approach to other families would be a significant fundamental contribution. A combination of experimental and computational efforts seems to be unavoidable (see, for example, refs 23,69, and 108), and advances on the computational side can be foreseen.

The opportunities in synthesis are most of all in demonstrating layered forms for other frameworks, that is, those so far known only in the complete 3D form. Basically any example is valuable, but some may be particularly significant. To date, the confirmed 2D zeolites are exclusively medium-pore or smaller zeolites. Obtaining an example of 12-ring zeolite is of high priority, especially like FAU or BEA. New 2D zeolite forms in addition to the 15 already identified also may be found.

So far, little attention has been paid to elucidation of the formation of 2D lamellar precursors. It is tacitly assumed to be caused by a “favorable” template that blocks adjacent layers from forming a covalent bond. The designed synthesis of layered MFI⁷² reinforces this concept. It was suggested² that Al-populated sites may play a significant role in the drive toward fully condensed (3D structures) since most layered precursors are silicates or low-Al materials. The exceptions to this may be readily explained, MCM-22 being a case in point: the layered precursor has Si/Al down to ~13/1 but the surface is largely populated by silanol groups, while Al atoms are assumed to be “buried” inside the layer (balancing the HMI templates). When the Al content increases, the completed 3D framework (MCM-49) is obtained directly. PREFER is another odd example: it nominally has Al, but it is a fluoride-based preparation and possibly subject to different assembly/formation rules. The curious Al-rich “exception” is NSI,²⁶¹ claimed to be prepared at quite low Si/Al ratio. There were not enough data (XRD) to assess the nature and quality of the high-Al-containing NSI precursor. It might be interesting material to study to gain insight into the above-proposed role of Al in promoting 3D connectivity.

The ADOR mechanism represents a new and intriguing approach to producing new zeolites via layered precursors that one can produce from other frameworks. It was the first case carried out starting from zeolite UTL. We should anticipate similar results with numerous other zeolites with D4R units containing Ge. The question is why this ADOR generalization should end with Ge and the cubic layer bridging units? Maybe other bridges can be enriched with Ge (zeolite NU-87) or other heteroatoms. Generally, anisotropic structures even containing silicon atoms in the direction of lowest density might be selectively removed to produce new layered precursors and then reassembled as new zeolite. Another interesting direction to follow is producing 2D zeolite forms more expanded than the initial one. In the case of UTL/PCR, it would be making ordered pillared structures with layers separated with larger

pillars than in UTL. This would require not only the synthesis of appropriate prototypes of “triple-four-rings” or larger units but also their regular introduction to the interlayer space followed by full condensation.

In the investigation of the adsorptive and catalytic properties of the 2D zeolite families, it can be said that we have barely scratched the surface. So far, mostly the standard approaches and concepts developed for zeolite as microporous 3D frameworks have been applied. An example of one of the main challenges is characterization of layer disorder and spatial orientation. Whether it is possible to accomplish this in a reliable and quantitative manner is a vital question. A related problem concerns the nature and geometrical properties of interlayer species like pillars. In most cases so far, pillars are considered as inert space filler, and the possibility of their activation is a real opportunity.

In the development and expansion of fundamental skills and knowledge of 2D zeolites, we cannot forget that practical exploitation is the ultimate goal. In that regard, traditional zeolites provide a formidable competition that must be transcended. One of the primary early obstacles will be overcoming the cost and labor associated with additional preparation steps. It may in fact be an impossible challenge. Two-dimensional zeolites that can be made in one-step synthesis are particularly attractive to avoid additional preparation steps. If their advantage above the standard ones is shown, the path to commercial use may become open. In that regard, MCM-56 is already available for systematic exploration.

The fundamental and practical challenges in the area of 2D zeolites include the following:

(1) Synthesis of other zeolites in the form of two-dimensional materials. The ultimate goal is the synthesis of all known structural types of zeolites as 2D ones.

(2) Understanding the reaction mechanisms providing 2D zeolites and driving forces to prepare them. This involves both direct synthesis of 2D zeolites as well as 3D to 2D postsynthetic treatment.

(3) Utilization of 2D zeolites to prepare new structural types of zeolites or novel expanded structures.

(4) Generalization of ADOR mechanism for other germanosilicates with D4R structural units. Finding conditions for this mechanism with zeolites not containing Ge is even more ambitious.

(5) Investigation of adsorption and catalytic potential of 2D zeolites. Maybe other properties like window effects for membranes could be proposed.

Perhaps the most important aspect of the potential impact of 2D zeolites is simply the fact that new types of material are imaginable.

AUTHOR INFORMATION

Notes

The authors declare no competing financial interest.

Biographies



Wieslaw J. Roth was employed for 21 years as a researcher at Mobil and ExxonMobil in Paulsboro and Clinton, NJ. He is currently an associate professor in the Faculty of Chemistry, Jagiellonian University in Krakow, Poland, and collaborates regularly as visiting scientist with the J. Heyrovský Institute of Physical Chemistry, Academy of Sciences of the Czech Republic. He was co-recipient of The Donald W. Breck Award of the International Zeolite Association for the “discovery of mesoporous molecular sieves” in 1994, the R&D 100 Award for Innovation, and The Thomas Alva Edison Patent Award in 2008. He is a graduate of the Technical University of Wrocław in Poland (M.S.) and Southern Illinois University at Carbondale (Ph.D.). Before joining Mobil R&D in 1988, he was a postdoctoral researcher and staff in Professor F. A. Cotton’s group at Texas A&M University in College Station.



Professor Petr Nachtigall completed his Ph.D. in 1995 at the University of Pittsburgh. He then moved to Prague, where he held a research position in the Academy of Sciences of Czech Republic (Institute of Physical Chemistry and later Institute of Organic Chemistry and Biochemistry). In 2010 he moved to the Faculty of Science at Charles University in Prague, where he is a professor and Head of Department at the Department of Physical and Macromolecular Chemistry. His research is focused on the theoretical investigation of surface properties of solids, related mainly to gas adsorption and catalytic processes involving microporous and nanostructured materials. He has coauthored about 120 research papers.



Russell Morris was born in St. Asaph, North Wales, and completed a D.Phil. at the University of Oxford. From 1991 to 1995 he was a postdoctoral researcher at the University of California Santa Barbara before returning to the United Kingdom to take up a position at the University of St. Andrews, where he is now Professor of Structural and Materials Chemistry. His research interests lie in the synthesis, characterization, and application of porous solids. Among his notable research successes are development of ionothermal synthesis, chiral induction of solids built from achiral precursors, characterisation of solids by microcrystal X-ray diffraction, and application of porous solids in medicine and biology, particularly for the delivery of biologically active gases such as nitric oxide. In addition, current interests also include the directed assembly of new families of zeolite catalysts and the development of new synthetic methods for hybrid magnetic solids. He is a Fellow of the Royal Society of Edinburgh and the Learned Society of Wales. He is a current Royal Society Industry Fellow and holds an EPSRC Senior Fellowship.



Professor Jiří Čejka was born in Roudnice nad Labem, former Czechoslovakia, in 1960. He studied at the Institute of Chemical Technology in Prague and received his Ph.D. at the J. Heyrovský Institute of Physical Chemistry and Electrochemistry in Prague in 1988. He spent 6 months as a postdoctoral researcher at the Technical University of Vienna under the supervision of Professor J. A. Lercher. Currently, he is head of the Department of Synthesis and Catalysis at J. Heyrovský Institute of Physical Chemistry in Prague and lectures on catalysis at the Faculty of Science, Charles University in Prague. In 2005 he chaired the 3rd FEZA Conference on Zeolites in Prague. He is the organizer of a number of workshops devoted to zeolites and molecular sieves and organizes annually the School of Molecular Sieves, focused on diverse aspects of their chemistry and applications. His research interests involve synthesis of zeolites and mesoporous and novel nanostructured materials, physical chemistry of sorption and catalysis, and investigation of the role of porous catalysts in

transformations of hydrocarbons and their derivatives. He is co-author of more than 220 research papers and co-editor of five books.

ACKNOWLEDGMENTS

W.J.R. acknowledges financial support provided in part by the National Science Centre (Poland) with a grant approved under DEC-2011/03/B/515/01551. P.N. and J.Č. acknowledge the Czech Science Foundation for the project of the Centre of Excellence (P106/12/G015). The research leading to these results has received also a partial funding for P.N. and J.Č. from the European Union Seventh Framework Programme (FP7/2007-2013) under grant agreement n°604307.

REFERENCES

- (1) Barrer, R. M. *Hydrothermal Chemistry of Zeolites*; Academic Press: London, 1982.
- (2) Roth, W. J. *Stud. Surf. Sci. Catal.* **2007**, *168*, 221.
- (3) Čejka, J.; Corma, A.; Zones, S. *Zeolites and Catalysis*; Wiley-VCH: Weinheim, Germany, 2010.
- (4) Corma, A. *Chem. Rev.* **1995**, *95*, 559.
- (5) Čejka, J.; Centi, G.; Perez-Pariente, J.; Roth, W. J. *Catal. Today* **2012**, *179*, 2.
- (6) Bejblová, M.; Procházková, D.; Čejka, J. *ChemSusChem* **2009**, *2*, 486.
- (7) Kubicka, D.; Kubickova, I.; Čejka, J. *Catal. Rev.* **2013**, *55*, 1.
- (8) Čejka, J.; Wichterlova, B. *Catal. Rev.* **2002**, *44*, 375.
- (9) Perego, C.; Ingallina, P. *Green Chem.* **2004**, *6*, 274.
- (10) Zones, S. I. *Microporous Mesoporous Mater.* **2011**, *144*, 1.
- (11) *Zeolites and Ordered Mesoporous Materials: Progress and Prospects*; Čejka, J., van Bekkum, H., Eds.; Studies in Surface Science and Catalysis, Vol. 157; Elsevier: Amsterdam, 2005.
- (12) McCusker, L. B.; Baerlocher, C. *Stud. Surf. Sci. Catal.* **2005**, *157*, 41.
- (13) Bellussi, G.; Carati, A.; Rizzo, C.; Millini, R. *Catal. Sci. Technol.* **2013**, *3*, 833.
- (14) Baerlocher, C.; McCusker, L. B.; Olson, D. H. *Atlas of Zeolite Framework Types*; Elsevier: Amsterdam, 2007; <http://www.iza-structure.org/>.
- (15) Treacy, M. M. J.; Rivin, I.; Balkovsky, E.; Randall, K. H.; Foster, M. D. *Microporous Mesoporous Mater.* **2004**, *74*, 121.
- (16) Thomas, J. M.; Klinowski, J. *Angew. Chem., Int. Ed.* **2007**, *46*, 7160.
- (17) Li, Y.; Yu, J. H.; Xu, R. R. *Angew. Chem., Int. Ed.* **2013**, *52*, 1673.
- (18) Morris, R. E. *Top. Catal.* **2010**, *53*, 1291.
- (19) Davis, M. E. *Chem. Mater.* **2014**, *26*, 239.
- (20) Szostak, R. *Molecular Sieves: Principles of Synthesis and Identification*; Blackie Academic and Professional: London, 1998.
- (21) Morris, R. E.; James, S. L. *Angew. Chem., Int. Ed.* **2013**, *52*, 2163.
- (22) Verheyen, E.; Joos, L.; Van Haverbeke, K.; Breynaert, E.; Kasian, N.; Gobechiya, E.; Houthoofd, K.; Martineau, C.; Hinterstein, M.; Taulelle, F.; Van Speybroeck, V.; Waroquier, M.; Bals, S.; Van Tendeloo, G.; Kirschhock, C. E. A.; Martens, J. A. *Nat. Mater.* **2012**, *11*, 1059.
- (23) Roth, W. J.; Nachtigall, P.; Morris, R. E.; Wheatley, P. S.; Seymour, V. R.; Ashbrook, S. E.; Chlubná, P.; Grajciar, L.; Položij, M.; Zukal, A.; Shvets, O.; Čejka, J. *Nat. Chem.* **2013**, *5*, 628.
- (24) Perez-Ramirez, J.; Christensen, C. H.; Egeblad, K.; Christensen, C. H.; Groen, J. C. *Chem. Soc. Rev.* **2008**, *37*, 2530.
- (25) Smith, J. V. *Chem. Rev.* **1988**, *88*, 149.
- (26) Roth, W. J.; Čejka, J. *Catal. Sci. Technol.* **2011**, *1*, 43.
- (27) Ramos, F. S. O.; De Pietre, M. K.; Pastore, H. O. *RSC Adv.* **2013**, *3*, 2084.
- (28) Shvets, O. V.; Nachtigall, P.; Roth, W. J.; Čejka, J. *Microporous Mesoporous Mater.* **2013**, *182*, 229.
- (29) Rubin, M. K.; Chu, P. (Mobil Oil Corp.). *Composition of synthetic porous crystalline material, its synthesis and use*. U.S. Patent 4,954,325, September 4, 1990.

- (30) Leonowicz, M. E.; Lawton, J. A.; Lawton, S. L.; Rubin, M. K. *Science* **1994**, *264*, 1910.
- (31) Marler, B.; Gies, H. *Eur. J. Mineral.* **2012**, *24*, 405.
- (32) Roth, W. J.; Gil, B.; Marszalek, B. *Catal. Today* **2013**, *10.1016/j.cattod.2013.09.032*. Available Online: Oct 23, 2013
- (33) Sun, J. L.; Bonneau, C.; Cantin, A.; Corma, A.; Diaz-Cabanás, M. J.; Moliner, M.; Zhang, D. L.; Li, M. R.; Zou, X. D. *Nature* **2009**, *458*, 1154.
- (34) Corma, A.; Diaz-Cabanás, M. J.; Jiang, J.; Afeworki, M.; Dorset, D. L.; Soled, S. L.; Strohmaier, K. G. *Proc. Natl. Acad. Sci. U.S.A.* **2010**, *107*, 13997.
- (35) Jiang, J. X.; Yu, J. H.; Corma, A. *Angew. Chem., Int. Ed.* **2010**, *49*, 3120.
- (36) Valtchev, V.; Majano, G.; Mintova, S.; Perez-Ramirez, J. *Chem. Soc. Rev.* **2013**, *42*, 263.
- (37) El-Roz, M.; Lakiss, L.; Vicente, A.; Bozhilov, K. N.; Thibault-Starzyk, F.; Valtchev, V. *Chem. Sci.* **2014**, *5*, 3.
- (38) Perez-Ramirez, J. *Nat. Chem.* **2012**, *4*, 250.
- (39) Michels, N. L.; Mitchell, S.; Milina, M.; Kunze, K.; Krumeich, F.; Marone, F.; Erdmann, M.; Marti, N.; Perez-Ramirez, J. *Adv. Funct. Mater.* **2012**, *22*, 2509.
- (40) Roth, W. J.; Dorset, D. L. *Microporous Mesoporous Mater.* **2011**, *142*, 32.
- (41) Bennett, J. M.; Chang, C. D.; Lawton, S. L.; Leonowicz, M. E.; Lissy, D. N.; Rubin, M. K. (Mobil Oil Corp.) *Synthetic porous crystalline MCM-49, its synthesis and use*. U.S. Patent 5,236,575, August 17, 1993.
- (42) Lawton, S. L.; Fung, A. S.; Kennedy, G. J.; Alemany, L. B.; Chang, C. D.; Hatzikos, G. H.; Lissy, D. N.; Rubin, M. K.; Timken, H. K. C.; Steuernagel, S.; Woessner, D. E. *J. Phys. Chem.* **1996**, *100*, 3788.
- (43) Roth, W. J.; Kresge, C. T.; Vartuli, J. C.; Leonowicz, M. E.; Fung, A. S.; McCullen, S. B. *Stud. Surf. Sci. Catal.* **1995**, *94*, 301.
- (44) Kresge, C. T.; Roth, W. J.; Simmons, K. G.; Vartuli, J. C. (Mobil Oil Corp.) *Crystalline oxide material*. U.S. Patent 5,229,341, July 20, 1993.
- (45) Fung, A. S.; Lawton, S. L.; Roth, W. J. (Mobil Oil Corp.) *Synthetic layered MCM-S6, its synthesis and use*. U.S. Patent 5,362,697, November 8, 1994.
- (46) Millini, R.; Perego, G.; Parker, W. O., Jr; Bellussi, G.; Carluccio, L. *Microporous Mater.* **1995**, *4*, 221.
- (47) Puppe, L.; Weisser, J. (Bayer Aktiengesellschaft) *Crystalline aluminosilicate PSH-3 and its process of preparation*. U.S. Patent 4,439,409, March 27, 1984.
- (48) Zones, S. I. (Chevron Research and Technology Co.) *New zeolite SSZ-25*. European Patent EP0231860, January 27, 1987.
- (49) Bellussi, G.; Perego, G.; Clerici, M. G.; Giusti, A. (Eniricerche S.p.A.) *Synthetic, crystalline, porous material containing oxides of silicon and boron*. European Patent EP0293032, November 5, 1988.
- (50) Graham, R. P. D. *Proc. Trans. R. Soc. Can.* **1918**, *12*, 185.
- (51) Schreyeck, L.; Caullet, P.; Mougenel, J. C.; Guth, J. L.; Marler, B. *J. Chem. Soc., Chem. Commun.* **1995**, 2187.
- (52) Schreyeck, L.; Caullet, P.; Mougenel, J. C.; Guth, J. L.; Marler, B. *Microporous Mater.* **1996**, *6*, 259.
- (53) Corma, A.; Diaz, U.; Domine, M. E.; Fornés, V. *Angew. Chem., Int. Ed.* **2000**, *39*, 1499.
- (54) Schoonheydt, R. A.; Pinnavaia, T.; Lagaly, G.; Gangas, N. *Pure Appl. Chem.* **1999**, *71*, 2367.
- (55) Vaughan, D. E. W. *Catal. Today* **1988**, *2*, 187.
- (56) Auerbach, S. M.; Carrado, K. A.; Dutta, P. K. *Handbook of Layered Materials*; Marcel Dekker, New York, 2004.
- (57) Geng, F. X.; Ma, R. Z.; Nakamura, A.; Akatsuka, K.; Ebina, Y.; Yamauchi, Y.; Miyamoto, N.; Tateyama, Y.; Sasaki, T. *Nat. Commun.* **2013**, *4*.
- (58) Roth, W. J.; Dorset, D. L.; Kennedy, G. J. *Microporous Mesoporous Mater.* **2011**, *142*, 168.
- (59) Roth, W. J. *Stud. Surf. Sci. Catal.* **2005**, *158*, 19.
- (60) Wang, L.; Liu, Y.; Xie, W.; Haihong, W.; Jiang, Y.; He, M.; Wu, P. *Stud. Surf. Sci. Catal.* **2007**, *170*, 635.
- (61) Wang, L. L.; Wang, Y.; Liu, Y. M.; Chen, L.; Cheng, S. F.; Gao, G. H.; He, M. Y.; Wu, P. *Microporous Mesoporous Mater.* **2008**, *113*, 435.
- (62) Fan, W. B.; Wu, P.; Namba, S.; Tatsumi, T. *Angew. Chem., Int. Ed.* **2004**, *43*, 236.
- (63) Wu, P.; Ruan, J. F.; Wang, L. L.; Wu, L. L.; Wang, Y.; Liu, Y. M.; Fan, W. B.; He, M. Y.; Terasaki, O.; Tatsumi, T. *J. Am. Chem. Soc.* **2008**, *130*, 8178.
- (64) Roth, W. J.; Dorset, D. L.; Kennedy, G. J.; Yorke, T.; Helton, T. E. *A novel molecular sieve composition EMM-12, a method of making and a process of using the same*. World Patent Appl. WO2010021795 (A1), February 25, 2010.
- (65) Corma, A.; Diaz, U.; Garcia, T.; Sastre, G.; Velty, A. *J. Am. Chem. Soc.* **2010**, *132*, 15011.
- (66) Corma, A.; Fornes, V.; Pergher, S. B.; Maesen, T. L. M.; Buglass, J. G. *Nature* **1998**, *396*, 353.
- (67) Varoon, K.; Zhang, X. Y.; Elyassi, B.; Brewer, D. D.; Gettel, M.; Kumar, S.; Lee, J. A.; Maheshwari, S.; Mittal, A.; Sung, C. Y.; Cococcioni, M.; Francis, L. F.; McCormick, A. V.; Mkhyan, K. A.; Tsapatsis, M. *Science* **2011**, *333*, 72.
- (68) Schweitzer, E. J. A.; van den Oosterkamp, P. F. *Microporous Mesoporous Mater.* **1998**, *20*, 397.
- (69) Zhang, X. Y.; Liu, D. X.; Xu, D. D.; Asahina, S.; Cychoz, K. A.; Agrawal, K. V.; Al Wahedi, Y.; Bhan, A.; Al Hashimi, S.; Terasaki, O.; Thommes, M.; Tsapatsis, M. *Science* **2012**, *336*, 1684.
- (70) Chlubna, P.; Roth, W. J.; Greer, H. F.; Zhou, W. Z.; Shvets, O.; Zukal, A.; Čejka, J.; Morris, R. E. *Chem. Mater.* **2013**, *25*, 542.
- (71) Roth, W. J.; Shvets, O. V.; Shamzhy, M.; Chlubna, P.; Kubu, M.; Nachtigall, P.; Čejka, J. *J. Am. Chem. Soc.* **2011**, *133*, 6130.
- (72) Choi, M.; Na, K.; Kim, J.; Sakamoto, Y.; Terasaki, O.; Ryoo, R. *Nature* **2009**, *461*, 246.
- (73) Millini, R.; Carluccio, L. C.; Carati, A.; Bellussi, G.; Perego, C.; Cruciani, G.; Zanardi, S. *Microporous Mesoporous Mater.* **2004**, *74*, 59.
- (74) Na, K.; Park, W.; Seo, Y.; Ryoo, R. *Chem. Mater.* **2011**, *23*, 1273.
- (75) Roth, W. J.; Dorset, D. L. *Struct. Chem.* **2010**, *21*, 385.
- (76) Treacy, M. M. J.; Vaughan, D. E. W.; Strohmaier, K. G.; Newsam, J. M. *Proc. R. Soc. A* **1996**, *452*, 813.
- (77) IZA structure commission web page, 2013: <http://www.iza-structure.org/>.
- (78) Andrews, S. J.; Papiz, M. Z.; McMeeking, R.; Blake, A. J.; Lowe, B. M.; Franklin, K. R.; Hellwell, J. R.; Harding, M. M. *Acta Crystallogr. B* **1988**, *44*, 73.
- (79) Zanardi, S.; Alberti, A.; Cruciani, G.; Corma, A.; Fornés, V.; Brunelli, M. *Angew. Chem., Int. Ed.* **2004**, *43*, 4933.
- (80) Marler, B.; Camblor, M. A.; Gies, H. *Microporous Mesoporous Mater.* **2006**, *90*, 87.
- (81) Roth, W. J.; Kresge, C. T. *Microporous Mesoporous Mater.* **2011**, *144*, 158.
- (82) Rollmann, L. D.; Schlenker, J. L.; Lawton, S. L.; Kennedy, C. L.; Kennedy, G. J. *Microporous Mesoporous Mater.* **2002**, *53*, 179.
- (83) Na, K.; Jo, C.; Kim, J.; Cho, K.; Jung, J.; Seo, Y.; Messinger, R. J.; Chmelka, B. F.; Ryoo, R. *Science* **2011**, *333*, 328.
- (84) Liebau, F. *Structural Chemistry of Silicates*; Springer-Verlag: Berlin, 1985.
- (85) Schwieger, W.; Lagaly, G. In *Handbook of Layered Materials*; Auerbach, S. M., Carrado, K. A., Dutta, P. K., Eds.; Marcel Dekker: New York, 2004, 541.
- (86) Ikeda, T.; Akiyama, Y.; Oumi, Y.; Kawai, A.; Mizukami, F. *Angew. Chem., Int. Ed.* **2004**, *43*, 4892.
- (87) Dorset, D. L.; Kennedy, G. J. *J. Phys. Chem. B* **2004**, *108*, 15216.
- (88) Zhao, Z. C.; Zhang, W. P.; Ren, P. J.; Han, X. W.; Muller, U.; Yilmaz, B.; Feyen, M.; Gies, H.; Xiao, F. S.; De Vos, D.; Tatsumi, T.; Bao, X. H. *Chem. Mater.* **2013**, *25*, 840.
- (89) Burton, A.; Accardi, R. J.; Lobo, R. F.; Falcioni, M.; Deem, M. W. *Chem. Mater.* **2000**, *12*, 2936.
- (90) Ikeda, T.; Kayamori, S.; Mizukami, F. *J. Mater. Chem.* **2009**, *19*, 5518.
- (91) Vortmann, S.; Rius, J.; Siegmann, S.; Gies, H. *J. Phys. Chem. B* **1997**, *101*, 1292.

- (92) Gies, H.; Marler, B.; Vortmann, S.; Oberhagemann, U.; Bayat, P.; Krink, K.; Rius, J.; Wolf, I.; Fyfe, C. *Microporous Mesoporous Mater.* **1998**, *21*, 183.
- (93) Marler, B.; Stroter, N.; Gies, H. *Microporous Mesoporous Mater.* **2005**, *83*, 201.
- (94) Kirchner, R. M.; Bennett, J. M. *Zeolites* **1994**, *14*, 523.
- (95) Wheatley, P. S.; Morris, R. E. *J. Mater. Chem.* **2006**, *16*, 1035.
- (96) Oliver, S.; Kuperman, A.; Ozin, G. A. *Angew. Chem., Int. Ed.* **1998**, *37*, 46.
- (97) Cundy, C. S.; Cox, P. A. *Chem. Rev.* **2003**, *103*, 663.
- (98) Cundy, C. S.; Cox, P. A. *Microporous Mesoporous Mater.* **2005**, *82*, 1.
- (99) Beck, J. S.; Vartuli, J. C.; Roth, W. J.; Leonowicz, M. E.; Kresge, C. T.; Schmitt, K. D.; Chu, C. T. W.; Olson, D. H.; Sheppard, E. W.; McCullen, S. B.; Higgins, J. B.; Schlenker, J. L. *J. Am. Chem. Soc.* **1992**, *114*, 10834.
- (100) Zhao, D.; Wan, Y.; Zhou, W. *Ordered Mesoporous Materials*; Wiley: New York, 2012.
- (101) Na, K.; Choi, M.; Park, W.; Sakamoto, Y.; Terasaki, O.; Ryoo, R. *J. Am. Chem. Soc.* **2010**, *132*, 4169.
- (102) Na, K.; Choi, M.; Ryoo, R. *Microporous Mesoporous Mater.* **2013**, *166*, 3.
- (103) Seo, Y.; Lee, S.; Jo, C.; Ryoo, R. *J. Am. Chem. Soc.* **2013**, *135*, 8806.
- (104) Park, W.; Yu, D.; Na, K.; Jelfs, K. E.; Slater, B.; Sakamoto, Y.; Ryoo, R. *Chem. Mater.* **2011**, *23*, 5131.
- (105) Dhainaut, J.; Daou, T. J.; Bidal, Y.; Bats, N.; Harbuzaru, B.; Lapisardi, G.; Chaumeil, H.; Defoin, A.; Rouleau, L.; Patarin, J. *CrystEngComm* **2013**, *15*, 3009.
- (106) Stacchiola, D.; Kaya, S.; Weissenrieder, J.; Kuhlenbeck, H.; Shaikhutdinov, S.; Freund, H.-J.; Sierka, M.; Todorova, T. K.; Sauer, J. *Angew. Chem., Int. Ed.* **2006**, *45*, 7636.
- (107) Loffler, D.; Uhlrich, J. J.; Baron, M.; Yang, B.; Yu, X.; Lichtenstein, L.; Heinke, L.; Buchner, C.; Heyde, M.; Shaikhutdinov, S.; Freund, H. J.; Wlodarczyk, R.; Sierka, M.; Sauer, J. *Phys. Rev. Lett.* **2010**, *105*.
- (108) Boscoboinik, J. A.; Yu, X.; Yang, B.; Fischer, F. D.; Wlodarczyk, R.; Sierka, M.; Shaikhutdinov, S.; Sauer, J.; Freund, H. J. *Angew. Chem., Int. Ed.* **2012**, *51*, 6005.
- (109) Corma, A.; Diaz-Cabanas, M. J.; Jorda, J. L.; Martinez, C.; Moliner, M. *Nature* **2006**, *443*, 842.
- (110) Corma, A.; Moliner, M.; Serra, J. M.; Serna, P.; Diaz-Cabanas, M. J.; Baumes, L. A. *Chem. Mater.* **2006**, *18*, 3287.
- (111) Corma, A.; Diaz-Cabanas, M. J.; Martinez, C.; Rey, F. *Stud. Surf. Sci. Catal.* **2008**, *174*, 1087.
- (112) Sastre, G.; Vidal-Moya, J. A.; Blasco, T.; Rius, J.; Jorda, J. L.; Navarro, M. T.; Rey, F.; Corma, A. *Angew. Chem., Int. Ed.* **2002**, *41*, 4722.
- (113) Vidal-Moya, J. A.; Blasco, T.; Rey, F.; Corma, A.; Puche, M. *Chem. Mater.* **2003**, *15*, 3961.
- (114) Blasco, T.; Corma, A.; Diaz-Cabanas, M. J.; Rey, F.; Rius, J.; Sastre, G.; Vidal-Moya, J. A. *J. Am. Chem. Soc.* **2004**, *126*, 13414.
- (115) Petkov, P. S.; Aleksandrov, H. A.; Valtchev, V.; Vayssilov, G. N. *Chem. Mater.* **2012**, *24*, 2509.
- (116) Liu, X. L.; Ravon, U.; Tuel, A. *Chem. Mater.* **2011**, *23*, 5052.
- (117) Gao, F. F.; Jaber, M.; Bozhilov, K.; Vicente, A.; Fernandez, C.; Valtchev, V. *J. Am. Chem. Soc.* **2009**, *131*, 16580.
- (118) Zwijnenburg, M. A.; Bromley, S. T.; Jansen, J. C.; Maschmeyer, T. *Microporous Mesoporous Mater.* **2004**, *73*, 171.
- (119) Shvets, O. V.; Shamzhy, M. V.; Yaremov, P. S.; Musilova, Z.; Prochazkova, D.; Čejka, J. *Chem. Mater.* **2011**, *23*, 2573.
- (120) Shamzhy, M. V.; Shvets, O. V.; Opanasenko, M. V.; Kurfirtova, L.; Kubicka, D.; Čejka, J. *ChemCatChem* **2013**, *5*, 1891.
- (121) Shamzhy, M. V.; Shvets, O. V.; Opanasenko, M. V.; Yaremov, P. S.; Sarkisyan, L. G.; Chlubna, P.; Zukal, A.; Marthala, V. R.; Hartmann, M.; Čejka, J. *J. Mater. Chem.* **2012**, *22*, 15793.
- (122) Ren, Y. J.; Xu, L.; Zhang, L. Y.; Wang, J. G.; Liu, Y. M.; He, M. Y.; Wu, P. *Pure Appl. Chem.* **2012**, *84*, 561.
- (123) Dawson, C. J.; Pope, M. A. B.; O'Keeffe, M.; Treacy, M. M. J. *Chem. Mater.* **2013**, *25*, 3816.
- (124) Roth, W. J. *Pol. J. Chem.* **2006**, *80*, 703.
- (125) Moteki, T.; Chaikittisilp, W.; Shimojima, A.; Okubo, T. *J. Am. Chem. Soc.* **2008**, *130*, 15780.
- (126) Oberhagemann, U.; Bayat, P.; Marler, B.; Gies, H.; Rius, J. *Angew. Chem., Int. Ed.* **1996**, *35*, 2869.
- (127) Moteki, T.; Chaikittisilp, W.; Sakamoto, Y.; Shimojima, A.; Okubo, T. *Chem. Mater.* **2011**, *23*, 3564.
- (128) Wang, Y.; Liu, Y. M.; Wang, L. L.; Wu, H. H.; Li, X. H.; He, M. Y.; Wu, P. *J. Phys. Chem. C* **2009**, *113*, 18753.
- (129) Zhang, B.; Ji, Y. J.; Wang, Z. D.; Liu, Y. M.; Sun, H. M.; Yang, W. M.; Wu, P. *Appl. Catal., A* **2012**, *443*, 103.
- (130) Grajcar, L.; Bludsky, O.; Roth, W. J.; Nachtigall, P. *Catal. Today* **2013**, *204*, 15.
- (131) Borowski, M.; Marler, B.; Gies, H. Z. *Kristallogr.* **2002**, *217*, 233.
- (132) Ohtsuka, K. *Chem. Mater.* **1997**, *9*, 2039.
- (133) Takabashi, N.; Hata, H.; Kuroda, K. *Chem. Mater.* **2011**, *23*, 266.
- (134) Fukuda, K.; Sato, J.; Saida, T.; Sugimoto, W.; Ebina, Y.; Shibata, T.; Osada, M.; Sasaki, T. *Inorg. Chem.* **2013**, *52*, 2280.
- (135) Maheshwari, S.; Jordan, E.; Kumar, S.; Bates, F. S.; Penn, R. L.; Shantz, D. F.; Tsapatsis, M. *J. Am. Chem. Soc.* **2008**, *130*, 1507.
- (136) Roth, W. J.; Vartuli, J. C. *Stud. Surf. Sci. Catal.* **2002**, *141*, 273.
- (137) Kresge, C. T.; Vartuli, J. C.; Roth, W. J.; Leonowicz, M. E. *Stud. Surf. Sci. Catal.* **2004**, *148*, 53.
- (138) Roth, W. J.; Vartuli, J. C.; Kresge, C. T. *Stud. Surf. Sci. Catal.* **2000**, *129*, 501.
- (139) Kresge, C. T.; Roth, W. J. *Chem. Soc. Rev.* **2013**, *42*, 3663.
- (140) Corma, A.; Diaz, U.; Fornes, V.; Guil, J. M.; Martinez-Triguero, J.; Creyghton, E. J. *J. Catal.* **2000**, *191*, 218.
- (141) Kruck, M.; Jaroniec, M.; Pena, M. L.; Rey, F. *Chem. Mater.* **2002**, *14*, 4434.
- (142) Chlubna, P.; Roth, W. J.; Zukal, A.; Kubu, M.; Pavlatova, J. *Catal. Today* **2012**, *179*, 35.
- (143) Roth, W. J.; Chlubna, P.; Kubu, M.; Vitvarova, D. *Catal. Today* **2013**, *204*, 8.
- (144) Frontera, P.; Testa, F.; Aiello, R.; Nagy, J. B. *Stud. Surf. Sci. Catal.* **2005**, *158*, 271.
- (145) Frontera, P.; Testa, F.; Aiello, R.; Candamano, S.; Nagy, J. B. *Microporous Mesoporous Mater.* **2007**, *106*, 107.
- (146) Wang, B. Y.; Wu, J. M.; Yuan, Z. Y.; Xiang, S. H. *Chin. J. Catal.* **2009**, *30*, 60.
- (147) Corma, A.; Fornes, V.; Diaz, U. *Chem. Commun.* **2001**, 2642.
- (148) Ogino, I.; Nigra, M. M.; Hwang, S. J.; Ha, J. M.; Rea, T.; Zones, S. I.; Katz, A. *J. Am. Chem. Soc.* **2011**, *133*, 3288.
- (149) Brenn, U.; Ernst, H.; Freude, D.; Herrmann, R.; Jähnig, R.; Karge, H. G.; Kärger, J.; König, T.; Mädler, B.; Pingel, U. T.; Prochnow, D.; Schwieger, W. *Microporous Mesoporous Mater.* **2000**, *40*, 43.
- (150) Kosuge, K.; Tsunashima, A. *J. Chem. Soc., Chem. Commun.* **1995**, 2427.
- (151) Takahashi, N.; Kuroda, K. *J. Mater. Chem.* **2011**, *21*, 14336.
- (152) Macedo, T. R.; Aioldi, C. *Microporous Mesoporous Mater.* **2010**, *128*, 158.
- (153) Osada, S.; Iribe, A.; Kuroda, K. *Chem. Lett.* **2013**, *42*, 80.
- (154) Ruan, J. F.; Wu, P.; Slater, B.; Terasaki, O. *Angew. Chem., Int. Ed.* **2005**, *44*, 6719.
- (155) Gies, H.; Muller, U.; Yilmaz, B.; Tatsumi, T.; Xie, B.; Xiao, F. S.; Bao, X. H.; Zhang, W. P.; De Vos, D. *Chem. Mater.* **2011**, *23*, 2545.
- (156) Asakura, Y.; Matsuo, Y.; Takahashi, N.; Kuroda, K. *Bull. Chem. Soc. Jpn.* **2011**, *84*, 968.
- (157) Ikeda, T.; Kayamori, S.; Oumi, Y.; Mizukami, F. *J. Phys. Chem. C* **2010**, *114*, 3466.
- (158) Xu, H.; Yang, B. T.; Jiang, J. G.; Jia, L. L.; He, M. Y.; Wu, P. *Microporous Mesoporous Mater.* **2013**, *169*, 88.
- (159) Ruan, J. F.; Wu, P.; Slater, B.; Zhao, Z. L.; Wu, L. L.; Terasaki, O. *Chem. Mater.* **2009**, *21*, 2904.

- (160) Fan, W. B.; Wu, P.; Namba, S.; Tatsumi, T. *J. Catal.* **2006**, *243*, 183.
- (161) Fan, W. B.; Wei, S. Q.; Yokoi, T.; Inagaki, S.; Li, J. F.; Wang, J. G.; Kondo, J. N.; Tatsumi, T. *J. Catal.* **2009**, *266*, 268.
- (162) Inagaki, S.; Imai, H.; Tsujuchi, S.; Yakushiji, H.; Yokoi, T.; Tatsumi, T. *Microporous Mesoporous Mater.* **2011**, *142*, 354.
- (163) Inagaki, S.; Tatsumi, T. *Chem. Commun.* **2009**, 2583.
- (164) Landis, M. E.; Aufdembrink, B. A.; Chu, P.; Johnson, I. D.; Kirker, G. W.; Rubin, M. K. *J. Am. Chem. Soc.* **1991**, *113*, 3189.
- (165) Barth, J. O.; Kornatowski, J.; Lercher, J. A. *J. Mater. Chem.* **2002**, *12*, 369.
- (166) Barth, J. O.; Jentys, A.; Kornatowski, J.; Lercher, J. A. *Chem. Mater.* **2004**, *16*, 724.
- (167) Kornatowski, J.; Barth, J. O.; Erdmann, K.; Rozwadowski, M. *Microporous Mesoporous Mater.* **2006**, *90*, 251.
- (168) Eilertsen, E. A.; Ogino, I.; Hwang, S. J.; Rea, T.; Yeh, S.; Zones, S. I.; Katz, A. *Chem. Mater.* **2011**, *23*, 5404.
- (169) Corma, A.; Fornes, V.; Guil, J. M.; Pergher, S.; Maesen, T. L. M.; Buglass, J. G. *Microporous Mesoporous Mater.* **2000**, *38*, 301.
- (170) Schenkel, R.; Barth, J. O.; Kornatowski, J.; Lercher, J. A. *Stud. Surf. Sci. Catal.* **2002**, *142*, 69.
- (171) Dorset, D. L.; Roth, W. J.; Gilmore, C. J. *Acta Crystallogr. A* **2005**, *61*, 516.
- (172) Narkhede, V. V.; Gies, H. *Chem. Mater.* **2009**, *21*, 4339.
- (173) Juttu, G. G.; Lobo, R. F. *Microporous Mesoporous Mater.* **2000**, *40*, 9.
- (174) Haag, W. O.; Lago, R. M.; Weisz, P. B. *Nature* **1984**, *309*, 589.
- (175) Cheng, J. C.; Fung, A. D.; Klocke, D. J.; Lawton, S. L.; Lissy, D. N.; Roth, W. J.; Smith, C. M.; Walsh, D. E. (Mobil Oil Corp.) *Process for preparing short chain alkyl aromatic compounds*. U.S. Patent 5,453,554 September 26, 1995.
- (176) Thommes, M. In *Characterization of Porous Solids and Powders: Surface Area, Pore Size and Density*; Lowell, S., Shields, J. E., Thommes, M., Eds.; Particle Technology Series; Kluwer: Dordrecht, The Netherlands, 2004.
- (177) Zubowa, H. L.; Schneider, M.; Schreier, E.; Eckelt, R.; Richter, M.; Fricke, R. *Microporous Mesoporous Mater.* **2008**, *109*, 317.
- (178) de Pietre, M. K.; Bonk, F. A.; Rettori, C.; Garcia, F. A.; Pastore, H. O. *Microporous Mesoporous Mater.* **2012**, *156*, 244.
- (179) Chica, A.; Diaz, U.; Fornés, V.; Corma, A. *Catal. Today* **2009**, *147*, 179.
- (180) Jacobson, A. J. *Mater. Sci. Forum* **1994**, *152–3*, 1.
- (181) Ma, R.; Sasaki, T. *Adv. Mater.* **2010**, *22*, 5082.
- (182) Climent, M. J.; Corma, A.; Velty, A. *Appl. Catal., A* **2004**, *263*, 155.
- (183) Palin, L.; Croce, G.; Viterbo, D.; Milanesio, M. *Chem. Mater.* **2011**, *23*, 4900.
- (184) Schlenker, J. L.; Peterson, B. K. *J. Appl. Crystallogr.* **1996**, *29*, 178.
- (185) Corma, A.; Diaz-Cabanas, M. J.; Moliner, M.; Martinez, C. J. *Catal.* **2006**, *241*, 312.
- (186) Kubů, M.; Roth, W. J.; Greer, H. F.; Zhou, W.; Morris, R. E.; Přech, J.; Čejka, J. *Chem.—Eur. J.* **2013**, *19*, 13937.
- (187) Goergen, S.; Fayad, E.; Laforgue, S.; Magnoux, P.; Rouleau, L.; Patarin, J. *J. Porous Mater.* **2011**, *18*, 639.
- (188) Nicolopoulos, S.; Gonzalez-Calbet, J. M.; Vallet-Regí, M.; Corma, A.; Corell, C.; Guil, J. M.; Perez-Pariente, J. *J. Am. Chem. Soc.* **1995**, *117*, 8947.
- (189) Pedone, A.; Malavasi, G.; Menziani, M. C.; Segre, U.; Musso, F.; Corno, M.; Civalleri, B.; Ugliengo, P. *Chem. Mater.* **2008**, *20*, 2522.
- (190) Cygan, R. T.; Liang, J. J.; Kalinichev, A. G. *J. Phys. Chem. B* **2004**, *108*, 1255.
- (191) Bushuev, Y. G.; Sastre, G. *J. Phys. Chem. C* **2009**, *113*, 10877.
- (192) Bushuev, Y. G.; Sastre, G. *J. Phys. Chem. C* **2011**, *115*, 21942.
- (193) Yang, B.; Kaden, W. E.; Yu, X.; Boscoboinik, J. A.; Martynova, Y.; Lichtenstein, L.; Heyde, M.; Sterrer, M.; Włodarczyk, R.; Sierka, M.; Sauer, J.; Shaikhutdinov, S.; Freund, H. J. *Phys. Chem. Chem. Phys.* **2012**, *14*, 11344.
- (194) Boscoboinik, J. A.; Yu, X.; Emmez, E.; Yang, B.; Shaikhutdinov, S.; Fischer, F. D.; Sauer, J.; Freund, H.-J. *J. Phys. Chem. C* **2013**, *117*, 13547.
- (195) Yang, B.; Emmez, E.; Kaden, W. E.; Yu, X.; Boscoboinik, J. A.; Sterrer, M.; Shaikhutdinov, S.; Freund, H. J. *J. Phys. Chem. C* **2013**, *117*, 8336.
- (196) Nachtigall, P.; Bludsky, O.; Grajcar, L.; Nachtigallova, D.; Delgado, M. R.; Arean, C. O. *Phys. Chem. Chem. Phys.* **2009**, *11*, 791.
- (197) Lee, K.; Murray, E. D.; Kong, L. Z.; Lundqvist, B. I.; Langreth, D. C. *Phys. Rev. B* **2010**, *82*, No. 081101.
- (198) Klimes, J.; Bowler, D. R.; Michaelides, A. *J. Phys.-Condens. Mater* **2010**, *22*, No. 022201.
- (199) Grimme, S. *J. Comput. Chem.* **2006**, *27*, 1787.
- (200) Rimola, A.; Costa, D.; Sodupe, M.; Lambert, J.-F.; Ugliengo, P. *Chem. Rev.* **2013**, *113*, 4216.
- (201) Tosoni, S.; Civalleri, B.; Ugliengo, P. *J. Phys. Chem. C* **2010**, *114*, 19984.
- (202) Hermann, J.; Trachta, M.; Nachtigall, P.; Bludsky, O. *Catal. Today* **2013**, *10.1016/j.cattod.2013.09.016*. Available Online: Oct 12, 2013
- (203) Bludsky, O.; Rubes, M.; Soldan, P.; Nachtigall, P. *J. Chem. Phys.* **2008**, *128*, No. 114102.
- (204) Hermann, J.; Bludsky, O. *J. Chem. Phys.* **2013**, *139*, No. 034115.
- (205) Seo, Y.; Cho, K.; Jung, Y.; Ryoo, R. *ACS Catal.* **2013**, *3*, 713.
- (206) Kim, W.; Kim, J. C.; Kim, J.; Seo, Y.; Ryoo, R. *ACS Catal.* **2013**, *3*, 192.
- (207) Park, H. J.; Heo, H. S.; Jeon, J. K.; Kim, J.; Ryoo, R.; Jeong, K. E.; Park, Y. K. *Appl. Catal., B* **2010**, *95*, 365.
- (208) Jo, C.; Ryoo, R.; Zilkova, N.; Vitvarova, D.; Čejka, J. *Catal. Sci. Technol.* **2013**, *3*, 2119.
- (209) Mehlhorn, D.; Valiullin, R.; Karger, J.; Cho, K.; Ryoo, R. *Microporous Mesoporous Mater.* **2012**, *164*, 273.
- (210) Koo, J. B.; Jiang, N.; Saravanamurugan, S.; Bejblova, M.; Musilova, Z.; Čejka, J.; Park, S. E. *J. Catal.* **2010**, *276*, 327.
- (211) Musilová, Z.; Žilková, N.; Park, S. E.; Čejka, J. *Top. Catal.* **2010**, *53*, 1457.
- (212) Diaz, U.; Cantin, A.; Corma, A. *Chem. Mater.* **2007**, *19*, 3686.
- (213) Chu, C. T.; Husain, A.; Huss, A., Jr.; Kresge, C. T.; Roth, W. J. (Mobil Oil Corp.) *Isoparaffin-olefin alkylation process with zeolite MCM-36*. U.S. Patent 5258569, November 2, 1993
- (214) He, Y. J.; Nivarthy, G. S.; Eder, F.; Seshan, K.; Lercher, J. A. *Microporous Mesoporous Mater.* **1998**, *25*, 207.
- (215) Maheshwari, S.; Martinez, C.; Portilla, M. T.; Llopis, F. J.; Corma, A.; Tsapatsis, M. *J. Catal.* **2010**, *272*, 298.
- (216) Cheng, J. C.; Fung, A. S.; Klocke, D. J.; Lawton, S. L.; Lissy, D. N.; Roth, W. J.; Smith, C. M.; Walsh, D. E. (Mobil Oil Corp.) *Process for preparing short-chain alkylaromatic compounds with a zeolite catalyst*. U.S. Patent 5,557,024, September 17, 1996.
- (217) Corma, A.; Martinez-Soria, V.; Schnoeveld, E. *J. Catal.* **2000**, *192*, 163.
- (218) Čejka, J.; Krejčí, A.; Žilková, N.; Kotrla, J.; Ernst, S.; Weber, A. *Microporous Mesoporous Mater.* **2002**, *53*, 121.
- (219) Wichterlova, B.; Čejka, J.; Žilkova, N. *Microporous Mater.* **1996**, *6*, 405.
- (220) Čejka, J.; Kapustin, G. A.; Wichterlova, B. *Appl. Catal., A* **1994**, *108*, 187.
- (221) Wichterlova, B.; Čejka, J. *J. Catal.* **1994**, *146*, 523.
- (222) Zilkova, N.; Shamzhy, M.; Shvets, O.; Čejka, J. *Catal. Today* **2013**, *204*, 22.
- (223) Davis, T. M.; Chen, C. Y.; Zilkova, N.; Vitvarova-Prochazkova, D.; Čejka, J.; Zones, S. I. *J. Catal.* **2013**, *298*, 84.
- (224) Laforgue, S.; Ayrault, P.; Manin, D.; Guisnet, M. *Appl. Catal., A* **2005**, *279*, 79.
- (225) Martinez, A.; Peris, E.; Sastre, G. *Catal. Today* **2005**, *107–108*, 676.
- (226) Corma, A.; Fornes, V.; Jordà, J. L.; Rey, F.; Fernandez-Lafuente, R.; Guisan, J. M.; Mateo, B. *Chem. Commun.* **2001**, 419.

- (227) Botella, P.; Corma, A.; Carr, R. H.; Mitchell, C. *J. Appl. Catal., A* **2011**, *398*, 143.
- (228) Botella, P.; Corma, A.; Mitchell, C. *Stud. Surf. Sci. Catal.* **2005**, *158*, 1263.
- (229) Concepcion, P.; Lopez, C.; Martinez, A.; Puntes, V. E. *J. Catal.* **2004**, *228*, 321.
- (230) Prieto, G.; Martinez, A.; Concepcion, P.; Moreno-Tost, R. J. *Catal.* **2009**, *266*, 129.
- (231) Martinez, A.; Lopez, C.; Marquez, F.; Diaz, I. *J. Catal.* **2003**, *220*, 486.
- (232) Da Costa-Serra, J. F.; Chica, A. *Int. J. Hydrogen Energy* **2011**, *36*, 3862.
- (233) Frontera, P.; Macario, A.; Aloise, A.; Antonucci, P. L.; Giordano, G.; Nagy, J. B. *Catal. Today* **2013**, *218–219*, 18.
- (234) Kim, J.; Park, W.; Ryoo, R. *ACS Catal.* **2011**, *1*, 337.
- (235) Koekkoek, A. J. J.; Kim, W.; Degirmenci, V.; Xin, H.; Ryoo, R.; Hensen, E. J. M. *J. Catal.* **2013**, *299*, 81.
- (236) Corma, A.; Diaz, U.; Fornes, V.; Jorda, J. L.; Domine, M.; Rey, F. *Chem. Commun.* **1999**, 779.
- (237) Corma, A.; Diaz, U.; Domine, M. E.; Fornes, V. *Chem. Commun.* **2000**, 137.
- (238) Kan, Q. B.; Fornes, V.; Rey, F.; Corma, A. *J. Mater. Chem.* **2000**, *10*, 993.
- (239) Corma, A.; Diaz, U.; Domine, M. E.; Fornes, V. *J. Am. Chem. Soc.* **2000**, *122*, 2804.
- (240) Wu, P.; Tatsumi, T. *Chem. Commun.* **2002**, 1026.
- (241) Wu, P.; Nuntasri, D.; Ruan, J. F.; Liu, Y. M.; He, M. Y.; Fan, W. B.; Terasaki, O.; Tatsumi, T. *J. Phys. Chem. B* **2004**, *108*, 19126.
- (242) Wu, P.; Tatsumi, T.; Komatsu, T.; Yashima, T. *J. Catal.* **2001**, *202*, 245.
- (243) Na, K.; Jo, C.; Kun, J.; Ahn, W. S.; Ryoo, R. *ACS Catal.* **2011**, *1*, 901.
- (244) Climent, M. J.; Corma, A.; Velty, A.; Susarte, M. *J. Catal.* **2000**, *196*, 345.
- (245) Climent, M. J.; Corma, A.; Iborra, S. *Chem. Rev.* **2011**, *111*, 1072.
- (246) Lima, S.; Pillinger, M.; Valente, A. A. *Catal. Commun.* **2008**, *9*, 2144.
- (247) Taguchi, A.; Schuth, F. *Microporous Mesoporous Mater.* **2005**, *77*, 1.
- (248) Martin-Aranda, R. M.; Čejka, J. *Top. Catal.* **2010**, *53*, 141.
- (249) Zukal, A.; Dominguez, I.; Mayerova, J.; Čejka, J. *Langmuir* **2009**, *25*, 10314.
- (250) Gonzalez-Arellano, C.; Corma, A.; Iglesias, M.; Sanchez, F. *Adv. Synth. Catal.* **2004**, *346*, 1758.
- (251) Corma, A.; Gutierrez-Puebla, E.; Iglesias, M.; Monge, A.; Perez-Ferreras, S.; Sanchez, F. *Adv. Synth. Catal.* **2006**, *348*, 1899.
- (252) Silveira, F.; Petry, C. F.; Pozebon, D.; Pergher, S. B.; Detoni, C.; Stedile, F. C.; dos Santos, J. H. Z. *Appl. Catal., A* **2007**, *333*, 96.
- (253) Corma, A.; Fornes, V.; Galletero, M. S.; Garcia, H.; Scaiano, J. C. *Chem. Commun.* **2002**, 334.
- (254) Corma, A.; Fornes, V.; Rey, F. *Adv. Mater.* **2002**, *14*, 71.
- (255) Dominguez, I.; Fornes, V.; Sabater, M. J. *J. Catal.* **2004**, *228*, 92.
- (256) Štěpnička, P.; Křečková, P.; Semler, M.; Čejka, J. *Z. Anorg. Allg. Chem.* **2014**, in press.
- (257) Mitchell, S.; Michels, N. L.; Perez-Ramirez, J. *Chem. Soc. Rev.* **2013**, *42*, 6094.
- (258) Mitchell, S.; Michels, N. L.; Kunze, K.; Pérez-Ramírez, J. *Nat. Chem.* **2012**, *4*, 825.
- (259) Vartuli, J. C.; Roth, W. J.; Degnan, T. F., Jr. In *Dekker Encyclopedia of Nanoscience and Nanotechnology*; Marcel Dekker: New York, 2004.
- (260) Dorset, D. L.; Roth, W. J. *Z. Kristallogr. Cryst. Mater.* **2011**, *226*, 254.
- (261) Galve, A.; Gorgojo, P.; Navascués, N.; Casado, C.; Téllez, C.; Coronas, J. *Microporous Mesoporous Mater.* **2011**, *145*, 211.
- (262) Argauer, R. J.; Landolt, G. R. (Mobil Oil Corp.) *Crystalline zeolite ZSM-5 and method of preparing the same*, U.S. Patent 3,702,886, November 14, 1972.
- (263) Araki, T. *Z. Kristallogr.* **1980**, *152*, 207.
- (264) Whittam, T. V. (Imperial Chemical Industries Plc) *Zeolites NU-6(1) and NU-6(2)*. U.S. Patent 4,397,825, August 9, 1983.
- (265) Wang, Y. X.; Gies, H.; Marler, B.; Muller, U. *Chem. Mater.* **2005**, *17*, 43.
- (266) Brooke, H. J. *Edinb. Philos. J.* **1822**, *6*, 112.
- (267) Thomson, T. J. *Nat. Philos., Chem., Arts* **1811**, *29*, 285.
- (268) Blake, A. J.; Franklin, K. R.; Lowe, B. M. *J. Chem. Soc., Dalton Trans.* **1988**, 2513.
- (269) Kresge, C. T.; Roth, W. J. (Mobil Oil Corp.) *Crystalline oxide material*. U.S. Patent 5,266,541, November 30, 1993.